Effect of Small Concentrations of Gallium and Lead on Anodic Activation of Aluminium in Chloride Solution

Esma Senel* and Kemal Nisancioglu**

Department of Materials Science and Engineering, Norwegian University of Science and Technology, N-7491 Trondheim, Norway

Abstract

The present objective is to investigate the combined effect of alloyed Pb and Ga on surface segregation by heat treatment and ensuing anodic activation of aluminium in chloride solution. Model alloys containing Pb and Ga, which were heat treated in the range 300-600°C, were characterised electrochemically in 5% NaCl solution. Annealing at 600°C resulted in significant segregation of Pb causing limited activation, while Ga remained in solid solution. The presence 50 ppm Ga had only a small contribution to activation, while 1000 ppm Ga contributed significantly by becoming enriched at areas around Pb segregations and spreading radially by dealloying.

* Present address: Hydro, 4265 Haavik, Norway
** Corresponding author kemaln@material.ntnu.no

Introduction

Lead and gallium are ubiquitous trace elements in commercial aluminium alloys, originating from the raw material bauxite [1-3]. While Pb is normally present at the ppm level by weight as a trace element in most commercial alloys, the Ga concentration is in the range 50 to 200 ppm. However, these elements may become enriched at the surface by orders of magnitude as a result of heat treatment and dealloying, respectively. The surface segregation of Pb by heat treatment of binary [4-7] and ternary [8-10] model alloys has been under investigation by this group, along with its role on anodic activation of the alloy in chloride media [11,12]. Anodic activation was defined as significant depression of the anodic breakdown (pitting) potential and significant increase in the anodic current density output in the potential range where aluminium is normally expected to be passive [12]. Solubility of Pb in solid Al is nearly zero [5], and its presence even at ppm level is sufficient to cause enrichment of the element at the surface by heat treatment at 600°C, giving anodic activation. Solubility of Ga in solid aluminium is significant. Trace element Ga is therefore stable in solid aluminium even at high temperatures. However, Ga can become enriched at the surface because of selective corrosion of Al (dealloying), such as during alkaline etching or anodic polarization in chloride solution. Ga enriched in this manner may activate aluminium anodically in chloride solution especially if its concentration exceeds 500 ppm in the binary alloy [13-15].

Anodic activation of model and commercial Al alloys by Pb occurred within a reasonable period of heat treatment time (1 h) at 600°C, a temperature significantly above the melting point of Pb [5]. The period of heat treatment required for similar level of activation at 600°C increased significantly with decreasing temperature. Activation was attributed to the formation of a continuous nanofilm of Pb, which was trapped at the aluminium metal –

γAl_2O_3 interface by diffusion of Pb to the surface and growth of γAl_2O_3 into the metal [6]. Most of the Pb in the alloy segregated in the form of nanosized, nearly spherical particles. These particles were either detached from the metal or did not contribute significantly to the metallic contact area between segregated Pb and the underlying Al matrix, a necessary condition for anodic activation. Pb segregated also at lower temperatures, but mostly in the form of nanoparticles.

Anodic activation caused by Pb in chloride solution was characterized by two oxidation peaks at the potentials of about -0.91 V_{SCE} and -0.88 V_{SCE} in the polarization curve of the AlPb alloy heat-treated at 600°C [4-7,10]. Each peak was related to superficial etching of the surface, causing multi-layered attack during potentiodynamic polarization [7]. The first layer of corrosion was attributed to the undermining of the thermally formed oxide film along the Pb nano-film [6,7]. The second layer was a result of crevice corrosion in the crevice formed between the undermined oxide and metal surface with acidified anolyte still present. Presence of these oxidation peaks in the anodic potentiodynamic polarization of Al alloys were shown to be a clear indication of the segregated Pb nanofilm at the Al metal-oxide interface. Activation by Pb was a temporary effect [6]. The surface passivated after the Pb nanolayer was destroyed by corrosion.

Investigation of the model AlPb alloys did not explain the observation that certain commercial alloys become anodically active by heat treatment at temperatures significantly lower than 600°C, *e.g.*, 450°C for alloy AA8006 [10,11,16], and attention was directed toward the possible additional presence of the lower melting point elements In [17], Sn [18,19], Bi [20] and Ga [21]. The elements Ga, Sn and In are known to be more effective than

Pb as activators [4,22-24]. This was attributed to their lower melting points than Pb and higher solubility of Al in these elements [18,25].

The theory, which is often referred to in explaining activation of aluminium by the low melting point elements in Group IIIA-VA, is the formation of a liquid phase alloy (amalgam) of the segregated element and aluminium, as is the case for Hg [26,27] and Ga [28,29]. According to this theory, Al corrodes by dissolving into the amalgam where it is in contact with it and oxidizing at the surface of the amalgam, where it is in contact with the ambient atmosphere. The amalgam wetting the surface of Al metal prevents its oxidation to recover the passivating oxide. Since the elements of the group other than Hg and Ga, have their melting points significantly higher than room temperature, melting point depression [30-32], known to occur with decreasing size of solid material to nanometre dimension, is invoked to justify the applicability of the theory to the higher melting point elements. Amalgamation theory for the activation effect of these elements was suggested to occur by melting point depression of the segregated nano-sized Pb film [6] and Sn particles [18], constituting a liquid phase amalgam with aluminium.

The presence of a second element that can contribute to melting point depression is also of concern. Combined presence of the trace elements Pb and Sn in the commercial alloy 8006 caused activation at 450°C (instead of 600°C for Pb alone) by segregation of a nanofilm, rich in both Pb and Sn, at the metal-oxide interface [33]. This was attributed to the lower melting point of the PbSn film than the melting points of Pb and Sn segregated alone. Combined presence of 1000 ppm Ga and 100 ppm Sn activated Al as a result of annealing at a lower temperature of 300°C even in the absence of chloride ions in the solution [34]. This was

attributed to the formation of a GaSnAl amalgam by dealloying of the Al component in aqueous solution.

Although Pb is probably the least effective activator of aluminium among the Group IIIA-VA elements, its presence together with other elements in the Group can cause higher activation of aluminium than expected from the single element alone. This may arise from synergistic effects, as demonstrated, *e.g.*, for the element pairs Pb-Sn [33] and Ga-Sn [34]. No information is available about the combined effect of Pb and Ga. The objective of this study is, therefore, to investigate whether Pb and Ga, when present together at small concentrations in model ternary alloys, can cause a similar synergistic increase in anodic activation of aluminium in relation to the effect of these elements when they are present alone in model binary aluminium alloys.

Experimental

Materials. Model ternary alloys were prepared by adding 50 and 1000 ppm of gallium and 50 ppm of lead to high purity aluminium by casting in chilled copper moulds. The alloys were denoted as AlGa50Pb50 and AlGa1000Pb50 based on their Pb and Ga content in ppm. The choice of alloy compositions was based on the earlier extensive work on the binary AlPb [4-11] and AlGa [21] alloys. The anodic activation of the Al surface caused by Pb was not significantly affected by the Pb concentration in the range 5 – 50 ppm. The cause of this was related to the segregation of a limited and constant amount of Pb in the form of a nanofilm by heat treatment at 600°C, and the rest of the Pb in the alloy segregated in the form of nearly spherical particles. While the film was the main cause of anodic activation, the contribution of the segregated particles was relatively small, as determined by anodic polarization

measurements in chloride solution. The upper extreme of 50 ppm was selected since the chemical and morphological characterization of the element becomes easier with increasing concentration. The presence of 50 ppm Ga alone did not change the electrochemical and corrosion properties of the binary alloy significantly in anodic polarization experiments, and Ga concentration had to be increased to 1000 ppm to observe appreciable changes in the electrochemical properties of the binary AlGa alloy. The effect of the intermediate concentrations for the binary alloy are demonstrated in detail elsewhere [21].

The cast alloys were scalped and cold rolled from 20 mm to a final thickness of approximately 2 mm. The compositions of the rolled samples were verified by glow discharge mass spectrometry (GD-MS). Samples were ground with SiC paper and polished metallographically to 1 μm diamond paste finish. "As-polished" samples were not treated any further. For the heat treated samples, the treatment was conducted for 1 h in the temperature range 300-600°C in an air-circulating furnace, followed by quenching in water.

Surface characterization. Elemental depth profiles of the samples were determined after heat treatment and electrochemical testing by glow discharge optical emission spectrometry (GD-OES), using a Horiba Jobin Yvon instrument in radio frequency (RF) mode with a standard 4 mm diameter copper anode. The measurements were quantified for Al and O by using the standards available for pure Al and certified oxide (CE 650) [35]. The data for Ga was calibrated by using the direct proportionality shown to exist between the known amount of gallium in the bulk and the measured intensity of Ga emission at concentration levels of interest [36]. The data was collected every 5 ms during sputtering. The sputtering rate was 70 nm/s in the metal and 40 nm/s in the oxide [37].

The surface morphology and microstructure of samples were characterized before and after electrochemical tests by using a field emission gun scanning electron microscope (FE-SEM) of type Zeiss Ultra 55, equipped with Inca (Oxford Instruments) energy dispersive X-ray spectroscopy (EDS) capability.

Electrochemistry. All specimens were degreased in acetone and ethanol before potentiodynamic polarization in stirred 5 wt% NaCl solution at 25°C, which was exposed to ambient air. Earlier work showed that the anodic current density was not affected significantly by the presence of dissolved oxygen in the solution [5,9]. The sample area exposed to the solution was 1.33 cm^2. The cell geometry, solution volume and the stirring rate in the solution were identical in all runs. Anodic polarization curves were measured with respect to saturated calomel reference electrode (SCE) at a sweep rate of 0.1 mV/s in the positive potential direction, starting 50 mV below the corrosion potential. Selection of the solution concentration and the sweep rate were based on a previous attempt to optimize these for best observation of the active behaviour, which is an unstable, time-dependent process [11]. Potentiostatic runs were performed at selected potentials to investigate the transient processes between active and passive conditions.

Change in the corrosion potential of alloys AlGa1000 and AlGa1000Pb50 were investigated for a period of 20 h in synthetic seawater (ASTM D1141-98), whose pH was adjusted to 3 by adding glacial acetic acid. This procedure has often been used in the past [4,5] to observe changes in the corrosion potential of binary alloys of Al and Group IIIA-VA elements, as the surface of the alloy was lightly and slowly etched layer by layer in the presence of a weak acid.

Results

SEM. No observable change occurred in the surface morphology of the alloys after heat treatment at 300°C and 450°C, as investigated by SEM. After annealing at 600°C, formation of γAl_2O_3 was verified by observation of its typical porous morphology [38] and segregated Pb particles of size less than 50 nm (not shown [5]).

GD-OES. Elemental depth profiles did not show any discernible Ga segregation on any of the two AlGaPb alloys investigated in any of the heat treatment temperatures used, in accordance with the high solubility of Ga in solid Al. No segregation of Pb was detected for the as-polished condition and after annealing at 300°C. The oxide thickness for both alloys was about 5 nm in the as-polished condition and after heat treatment at this temperature [39]. After annealing at 450°C, Pb peak appeared at the metal-oxide interface of both alloys, as shown in Fig. 1a for alloy AlGa50Pb50 and Fig. 1b for alloy AlGa1000Pb50, while the Ga depth profile still remained uniform. The oxide thickness obtained was about 20 nm at this temperature, as determined by assuming that the position of the Pb peak corresponded to the oxide-metal interface [4]. The size of the Pb peak increased by heat treatment at 600°C for both alloys, as shown in Fig. 1c for alloy AlGa1000Pb50, and the oxide thickness became about 50 nm. The results for alloy AlGa50Pb50 (not shown [39]) were similar to those for AlGa1000Pb50 under identical conditions except for the obvious difference in the bulk Ga concentrations. The GD-OES data for heat treatment at 600°C agreed well with the earlier data for binary model AlPb alloys [4,5], indicating that the observed effect of heat treatment was determined by segregation of the trace element Pb. Area under the Pb enrichment curves were identical for both alloys at each annealing temperature [39] indicating that Ga, still in solid solution with Al, had no effect on the thermal segregation of Pb.

Electrochemistry. Figure 2 shows potentiodynamic polarization curves for the binary and ternary alloys in the as-polished condition (Fig. 2a) and after heat treatment at 300°C (Fig. 2b) and 600°C (Fig. 2c). Figure 2c includes also curves for alloy AlGa50Pb50 and AlGa1000Pb50 heat treated at 450°C. The polarization curves for alloys AlGa50, AlPb50 and AlGa50Pb50 showed nearly common critical breakdown potential of about -0.75 V_{SCE} in the as-polished condition (Fig. 2a), quite similar to that for pure Al. The differences observed below the critical breakdown potential, *i.e.*, the passive state was not reproducible. This was firstly due to the time dependence of the polarization curves, attributed to dealloying. Moreover, since the main interest was the anodic behaviour (activation), precautions for measurement of small currents were not taken, and dissolved oxygen was present in the solution, as also discussed in the experimental section. The curve for alloy AlGa1000 showed a slight, but clear, shift in the negative potential direction by about 50-100 mV relative to the curve for alloy AlGa50 in all conditions. The effect of Ga content on the anodic behaviour of the binary AlGa is discussed in more detail elsewhere [21]. Heat treatment at 300°C did not give a significant effect relative to the as-polished condition. This is in agreement with the GD-OES data, which did not indicate significant difference between the elemental depth profiles of the two conditions [39].

Heat treatment at 450°C gave only a slight increase in the activation of alloys AlGa50Pb50 and AlGa1000Pb50 relative to the 300°C condition (Fig. 2b), which was attributed to Pb segregation during annealing at 450°C, as shown by the GD-OES depth profile in Fig. 1a. However, the activation obtained by heat treatment at 600°C was significant (Fig. 2c) in accordance with the mechanism described in Introduction and earlier work in detail [4,5], *i.e.*, in the form of both continuous nanofilm and discrete particles. The added presence of 1000 ppm Ga caused increase in the activation by mainly increasing the current density output.

Corrosion potential data as a function of immersion time in acidified seawater for alloys AlGa1000 and AlGa1000Pb50, identically heat treated at 600°C, are shown in Fig. 3. Alloy AlGa1000 showed a significant increase in its corrosion potential at the outset, from a minimum of about -1.0 V_{SCE} to a fairly stable -0.83 V_{SCE} within a period of about 3 h. This value was only slightly more negative than the breakdown potential of the alloy (Fig. 2c), but appreciably more negative than the breakdown potential of pure Al. The corrosion potential of alloy AlGa1000Pb50 was similar to that of alloy AlGa1000 at the outset, but it stabilised at a significantly more negative value of about -0.97 V_{SCE}, which is comparable to its breakdown potential measured by potentiodynamic polarization (Fig. 2c).

Potentiostatic tests. Two potentials levels of about -0.8 V_{SCE} and -0.9 V_{SCE} were selected based on the potentiodynamic data to study time-dependent activation and passivation phenomena. These potentials are essentially close to the minima observed in Fig. 2c on the anodic potentiodynamic curves for 600°C-annealed alloys containing Pb. At -0.8 V_{SCE}, most alloy-heat treatment combinations showed some degree of activation to make comparison possible (Fig. 4a and 4b). AlGa binary alloys were passive below this potential at all heat-treatment conditions (Fig. 2). Alloy AlGa50Pb50, heat-treated at 300°C, showed passive behaviour at the applied potential, as indicated by anodic current density output at $\mu A/cm^2$ level in Fig. 4a. A similar result was obtained for the binary alloy AlGa treated identically [21]. The current density level became higher with increasing annealing temperature at a given time of polarization. For all annealing temperatures, the current density went through a maximum before decaying to a much lower steady-state level. With reference to the anodic behaviour of the binary AlGa [21] and AlPb [4,5,7] alloys, increased activation of alloy AlGa50Pb50 at the outset (the peak current density) with increasing heat treatment

temperature was attributed to segregation of Pb at the metal-oxide interface during annealing, as also indicated by the present GD-OES data (Fig. 1). However, the binary AlGa50 alloy, when annealed in the temperature range 300-600°C, was passive at -0.8 V_{SCE} [21]. In the case of AlPb alloys, passivation occurred after temporary active behaviour at the outset (decreasing current density following the peak) [5] as the Pb active layer, segregated at the metal-oxide interface by heat treatment, was removed by corrosion. Therefore, the initial active behaviour in Fig. 4a (the peak) is attributed to Pb segregated by heat treatment, and increasing steady-state current density with increasing annealing temperature is attributed to Ga enrichment by dealloying.

In the case of alloy AlGa1000Pb50, the current density at identical conditions increased with time for all heat-treatment temperatures, as shown in Fig. 4b. The sample annealed at 600°C gave the highest current density initially. The current density remained quite stable for about 30 min before increasing gradually as a function of time. Maintenance of active current density levels after prolonged polarization was attributed to high Ga content of the alloy, with reference to the anodic behaviour of the binary alloy AlGa1000 [21], which is also shown in Fig 4b for the annealing temperature of 300°C. High Ga content maintained AlGa1000Pb50 alloys (at all heat treatment conditions) in the active state with high current densities, while all AlGa50Pb50 alloys passivated after short active behaviour at the outset. The current density for the AlGa1000Ga50 samples, annealed at 300°C and 450°C, was lower than those annealed at 600°C at the outset. The current density for all cases then increased gradually to a similar level of about 65 mA/cm^2 after 4 h of polarisation.

At the more negative potential of -0.9 V_{SCE}, the binary alloy AlGa1000 was passive. The current density of alloy AlGa1000Pb50 (annealed at 300°C), initially at 0.1 mA/cm^2,

increased to about 30 mA/cm^2 within 2 h of exposure, as shown in Fig. 4c. Conversely, the same alloy, annealed at 600°C, was initially active at a current density of 7.5 mA/cm^2 at this potential, and it decreased to a lower level of 0.2 mA/cm^2 after 10 min. Alloy AlGa50Pb50, annealed at 300°C, was not as active as alloy AlGa1000Pb50 because of its low Ga content. However, it was more active than alloy AlGa1000. These differences between the annealing temperatures of 300°C and 600°C will be discussed further in the Discussion section.

Pb containing binary and ternary alloys, annealed at 600°C, were polarized at potentials -0.93 V_{SCE} (Fig. 5a) and -0.88 V_{SCE} (Fig. 5b), corresponding to the two oxidation peaks typically measured during potentiodynamic polarization of identically-treated Pb containing alloys (Fig. 2c). At -0.93 V_{SCE}, the current density attained a maximum of about 3 mA/cm^2 after about 1 min for alloys AlPb50 and AlGa50Pb50, while alloy AlGa1000Pb50 attained a maximum current density of about 7 mA/cm^2 after 8 s, as shown in Fig. 5a. The samples then passivated to a current density level of about 0.15 mA/cm^2 after 5 min for alloys AlPb50 and AlGa50Pb50 and after 10 min for alloy AlGa1000Pb50. At -0.88 V_{SCE}, two successive peaks were observed in the current transients of the three Pb containing alloys, as shown in Fig. 5b. The current transients for alloys AlPb50 and AlGa50Pb50 were similar. The peaks are believed to correspond to the corrosion mechanisms related to the peaks on the potentiodynamic polarization curves (Fig. 2c), as discussed in detail earlier for the binary alloy AlPb [7] and reviewed in the next section and Introduction. The trend in the current transient for alloy AlGa1000Pb50 was similar to that of alloys AlPb50 and AlGa50Pb50. However, the current density level was higher. The charge passed during polarisation at -0.88 V_{SCE}, until passivation occurred, was about 2 times higher for AlGa1000Pb50 than the other two alloys.

Corrosion morphology: 600ºC-annealed specimens. Corrosion behaviour of alloy AlGa50Pb50, annealed at 600°C, during potentiodynamic polarization was nearly identical to the well-documented behaviour of the binary AlPb alloys [5-7]. In summary, the surface was passive below the corrosion potential. The γAl_2O_3 layer was undermined nearly completely as a result of superficial etching following the Pb nanofilm present at metal-oxide interface on specimens annealed at 600°C, as the first anodic peak was formed. However, the film remained loosely attached to the surface, forming a crevice. The second layer, corresponding to the second anodic peak, occurred in the form of crevice corrosion. Each layer of corrosion was accompanied by hydrogen evolution and followed by relative passivity indicated by termination of the etching process and hydrogen evolution.

During polarisation of alloy AlGa1000Pb50 (annealed at 600°C), the first layer of corrosion was similar to that on alloy AlPb50 and AlGa50Pb50. However, pitting also occurred with intensive hydrogen evolution. Although undermining of the film spread over most of the exposed area as on alloy AlGa50Pb50 with resulting passivation of the etched area, pits continued to propagate. Pitting resulted in higher current density for alloy AlGa1000Pb50 in the polarisation curve in Fig. 2c, as well as in the potentiostatic polarisation data in Fig. 5a and 5b, in relation to alloy AlGa50Pb50. The focus in the remainder of this section is the corrosion of alloy AlGa1000Pb50.

Potentiodynamic polarization of AlGa1000Pb50 samples annealed at 600°C was terminated at predetermined potentials, and the resulting corrosion morphology of the sample was investigated *ex-situ* by FE-SEM. Fig. 6 shows corrosion morphologies obtained by sweeping the potential up to -0.93 V_{SCE}, which corresponded to the first oxidation peak in Fig. 2c. Fig. 6a shows a general view at low magnification. The slip planes seen were probably formed by

internal stresses introduced by water quenching after heat treatment [37]. The light grey areas, marked A, remained uncorroded at this potential. The dark grey areas, marked B, were formed by superficial etching along the metal-oxide interface, undermining the thermally-formed γAl_2O_3 layer [7]. Areas marked by white squares in Fig. 6a are shown at higher magnification in Fig. 6b-e. The propagation front under the oxide, seen in Fig. 6b, was not affected by the grain boundary (line with bright contrast). The undermined oxide and the etched surface, probably exposed by removal of part of the loosely attached film during rinsing of the sample after the run, is seen more clearly in Fig. 6c. Ga could not be detected by EDS at the surface. However, Pb particles were detected as bright spots in the back-scattered image (Fig. 6e) of the corroded area shown in Fig. 6d.

An AlGa1000Pb50 sample polarized up to -0.92 V_{SCE}, which corresponded to the minimum between the two oxidation curves in Fig. 2c. At this potential, the first layer of attack, which consisted of undermining of the oxide, covered most of the surface exposed to corrosion. The undermined oxide began to be detached locally from the surface during polarization, as shown in Fig. 7. The corroded metal with etched morphology (light grey), marked as C in the figure, also showed crystallographic pitting. This is in contrast to the pitting of the binary alloys and alloy AlGa50Pb50, which initiated at higher potentials close to the pitting potential of pure Al (Fig. 2c). As the undermined oxide was removed from the surface, corrosion continued propagating by forming crystallographic pits instead of passivation of the entire surface as was the case for the binary alloys and alloy AlGa50Pb50.

The corrosion morphology obtained by potentiostatic polarization at -0.88 V_{SCE} was similar to that shown in Fig. 7. Most of the undermined oxide was detached from the surface,

revealing crystallographic etching. Crystallographic pits were also observed on the etched surface, as shown in Fig. 7. EDS analysis did not indicate any Pb or Ga segregation.

Corrosion morphology: 300ºC-annealed and as-polished specimens. The analysis of corroded samples, heat-treated at 300°C, is limited to alloy AlGa1000Pb50, which was significantly more active than the other alloys annealed at this temperature. This alloy remained active after potentiostatic polarization for 2 h at -0.9 V_{SCE} (Fig. 4c). Corrosion morphology obtained after polarization is shown in Fig. 8a and 8b at different magnifications. The attack was in the grains rather than at grain boundaries. It was deeper and localized in contrast to the superficial etching of the sample annealed at 600°C. Ga was detected by EDS of the marked spot in Fig. 8c, as shown by the spectrum attached to the figure.

GD-OES Analysis of Corroded Surfaces. GD-OES analysis of samples, which were heat-treated at 600°C and polarized potentiostatically for 10 min at -0.93 V_{SCE}, revealed similar depth profiles for Pb on alloys AlPb50, AlGa50Pb50 and AlGa1000Pb50, with enrichment peak for Pb at a depth of about 125 nm, as shown for alloy AlGa1000Pb50 in Fig.9a. No Ga segregation could be detected. Judging from the inflection and intersection points of the O and Al profiles this time, instead of the location of the Pb peak as in the GD-OES results for the uncorroded specimens above, and considering the increased roughness of the surface, the thickness of the undermined oxide must be about the same as the thickness of γAl_2O_3 on as-heat treated, uncorroded samples (*cf.* Fig. 1c). The deeper position of the Pb peak, in relation to the as heat-treated surface, is probably determined by the remnants of Pb film, originally at the metal-oxide interface, collecting in the form of particles on etched aluminium metal surface, as discussed earlier [5]. The location of Pb at 125 nm should include the crevice height formed by undermining of the oxide [7].

GD-OES depth profiles of the same alloys, polarised at -0.88 V_{SCE}, is shown for alloy AlGa1000Pb50 in Fig. 9b, indicating that Pb enrichment was much closer to the surface, at a depth of a few nm. This resulted from the removal of the thermally formed oxide nearly completely from the sample surface (Fig. 7). Ga was also enriched, especially on alloy AlGa1000Pb50, as seen in Fig. 9b. The Ga peak was higher than the Pb peak. Otherwise, the Ga concentration followed the depth profile of Pb.

Depth profile of alloy AlGa1000Pb50, annealed at 300°C and potentiostatically polarised at -0.8 V_{SCE} is shown, in Fig. 9c. The figure indicates that the surface was enriched with Ga within a broader region of about 20 nm. Broadening was caused by surface roughness, which was higher than the surface annealed at 600°C, as indicated by Fig. 8. Pb profile was similar to that for the as-annealed (uncorroded) condition, only slightly enriched above the noise level at the surface.

To summarize some of the results above, enrichment of Ga and Pb was calculated from the area under the GD-OES profiles for as-annealed and as-corroded conditions of alloy AlGa1000Pb50, as shown in Fig. 10. Pb enrichment increased with increasing annealing temperature for 1 h of annealing time used, while the Ga concentration remained constant at its homogenised bulk concentration. However, the amount of Pb remaining at the surface of the sample (annealed at 600°C) after potentiostatic polarisation at -0.8 V_{SCE} was smaller than that for the as-annealed (uncorroded) state, while Ga was enriched. The amount of charge passed, for samples annealed at 300 and 600°C, during polarisation for 10 min was about the same at 17 and 18 C/cm^2, respectively. These results verify that Pb segregation by heat treatment, which increased with annealing temperature, did not affect the stability of Ga in

solid solution with Al. Ga became segregated by dealloying during corrosion, albeit affected by the amount and state of Pb already present due to segregation during heat treatment. Although an appreciable amount of segregated Pb was removed by corrosion, its contribution to the dealloying process, resulting in significant Ga enrichment is evident from these results.

Discussion

In the presence of Ga alone in Al, significant activation occurs only for sufficiently high Ga concentration, *viz.*, about 1000 ppm [13,14,21]. However, this took place after a certain induction period in potentiostatic testing for passivity breakdown to occur, if the underlying oxide was not destroyed by other means, such as mechanical damage. Breakdown with Ga alone required segregation of sufficient Ga by dealloying of the more active component Al in chloride solution (Ref. 21 and Fig. 4b above), depending on the applied potential. While activation occurred after an induction period of 8 min at -0.8 V_{SCE} (Fig. 4b), the surface remained passive for a much longer period at -0.9 V_{SCE} (Fig. 4c).

The role of added presence of Pb was to cause activation from the start of the experiment at increasing rate with increasing annealing temperature, according to the mechanism summarized in Introduction and Results (section on Corrosion Morphology: 600°C) and discussed in more detail in Ref. [7]. The initial activation is thus attributed to *a priori* presence of Pb, which segregated by heat treatment. This occurred only in particulate form at temperatures lower than 600°C. Despite particulate Pb causes limited activation at the outset, it appears to be sufficient to cause appreciable liquid Ga enrichment by dealloying of Al. The enriched Ga then starts contributing to the activation of the surface at an increasing degree with respect to time of potentiostatic polarization, as is evident from the curves for 300°C and

450°C in Fig. 4b (and Fig. 4c for alloy AlGa1000Pb50, annealed at 300°C). This difference between samples alloyed at 600°C and at the lower temperatures is attributed to the nature of Pb near the surface. Heat treatment at 600°C causes Pb segregation in the form of nearly continuous nanofilm at the metal-oxide interface causing significant activation from the outset of potentiostatic polarisation. Segregation in the form of film depletes Pb in the near surface region, thereby causing decrease in activation with large time of polarisation. Annealing at 450 and 300°C causes increasingly limited particulate segregation with decreasing temperature. Also due to limited wetting of the Al substrate in particulate form, activation caused at these temperatures is lower at the outset compared to the samples annealed at 600°C. However, the near surface region is not depleted of Pb by annealing at the lower temperatures. Subsequent sustained enrichment of Pb by dealloying during potentiostatic polarisation of these samples causes eventually a higher level of activation relative to the 600°C-annealed samples.

During potentiostatic polarisation involving prolonged exposure, removal of the interfacial film after a few minutes causes a decrease in the corrosion rate until the amount of Ga, needed to sustain the active surface state, becomes enriched at the surface by dealloying (Fig. 4b). This also depends on the applied potential as the driving force. While an increase is observed after a shallow minimum in the current density at an applied potential of -0.8 V_{SCE} for alloy AlGa1000Pb50, the current density increases again due to Ga enrichment. A similar recovery of current density does not appear to occur at a lower applied potential of -0.9 V_{SCE} (Fig. 4b). With further decrease in the applied potential, all Pb-containing alloys showed tendency for passivation as the activating Pb film was removed, and the driving force was not high enough to cause sufficient Ga enrichment by dealloying (Fig. 5). The apparent absence of Ga according to GD-OES analysis of a 600°C-annealed sample, corroded

potentiostatically at -0.93 V_{SCE}, can be attributed to this effect. In contrast, Ga was detected by EDS on samples corroded at -0.9 V_{SCE}. This result is related to the nature of Pb segregation by heat treatment and its effect on Ga enrichment by dealloying. Detection of enriched Ga can be elusive because of its rapid diffusion back into the bulk of Al alloy in the period between the electrochemical test and *ex situ* surface analysis [36].

For alloy AlGa50Pb50, the initial activation observed during potentiostatic runs (Fig. 4a) is due only to Pb segregated by heat treatment. However, activation cannot be maintained by subsequent enrichment of Ga by dealloying because the Ga content of the alloy is not sufficient for this. Passivation occurs after a short period of polarisation, as the Pb segregated by heat treatment is removed by corrosion. Segregation of Pb by dealloying is not significant either because the near-surface region becomes nearly depleted of Pb by thermal segregation [40].

The foregoing discussion is suggested also by the corrosion potential data for alloys annealed at 600°C in acidified synthetic seawater (Fig. 3). This solution was selected for the corrosion potential (E_{corr}) measurements because the evolution of the mixed potential can be observed as the removal of the surface layers occurs in an accelerated fashion [4,5]. We interpret stable E_{corr} for the AlGa1000 binary alloy close to its breakdown potential at about -0.83 V_{SCE} as limited activation (or reduced passivation) as a result of limited dealloying in the absence of Pb. E_{corr} exhibited by alloy AlGa1000Pb50 at a significantly more negative level (-0.97 V_{SCE}) than that for alloy AlGa1000 demonstrates activation of the surface from the outset due to presence of segregated Pb film. The sustainability of the negative potential at large times of immersion is due to Ga enrichment by dealloying of the Al component enhanced by segregation of Pb. These results demonstrate also the synergistic activation mechanism of Pb

and Ga acting together. The nature of Pb enrichment as a result of dealloying of Al in aqueous media has not been investigated in as much detail as Pb segregation by heat treatment.

Corrosion morphology obtained by polarisation of alloy AlGa1000Pb50 (annealed at 300°C) by potentiostatic polarisation at -0.9 V_{SCE} (Fig. 8) indicated tendency for cellular attack as discussed in Ref. 21 for binary AlGa alloys. Such morphology was attributed to formation of a GaAl liquid-phase alloy (amalgam) by dealloying of Ga and its stepwise spreading in the radial direction, autocatalytically activating the surface. On alloy AlGa1000Pb50, segregated insoluble Pb particles on the surface probably contributed to passivity breakdown and resulted in a more irregular propagation than on the AlGa binary alloy, both in depth and superficially, depending on the location of the segregations.

Alloy AlGa1000Pb50, annealed at 600°C, showed pitting corrosion, as well as superficial etching undermining the thermally formed γ-Al_2O_3 oxide (Fig. 8), well below the pitting potential of pure Al, while AlPb50 and AlGa50Pb50 exhibited only superficial etching of the active layer during potentiodynamic and potentiostatic polarisation. Alloy AlGa1000Pb50 did not passivate between the two characteristic steps of multilayer corrosion [7] due to sustained activation caused by Ga enrichment. The two characteristic oxidation peaks at -0.93 and -0.88 V_{SCE} were still present on the anodic polarisation curves of alloys AlPb50 and AlGa50Pb50 with the region of quasi-passivity between the two peaks (Fig. 2c).

Melting point depression of segregated Pb in form of nano-sized particles or interfacial film of nanometre thickness [30-32] was suggested to have a possible role on the formation of a liquid phase alloy with Al as the cause of anodic activation [6]. Dissolution of the Pb film or

particles in liquid Ga, which segregates by dealloying, may form a GaPb liquid alloy at nano-scale, with a much lower melting point than the bulk alloy [41]. Such an effect may be speculated to play a role in increased activation of the ternary alloy AlGa1000Pb50 in relation to the binary AlPb and AlGa alloys.

The present results are applicable only to model alloys AlPb, AlGa and AlGaPb prepared from their pure components. Commercial alloys, which in addition often contain Si and the noble transition elements Fe, Mn, Cu and Zn, are not as susceptible to anodic activation by Pb, as demonstrated in Ref. [9]. These elements, especially Cu, tend to counter the activating effect of Pb by ennobling the alloy surface in chloride solution. The same appears to be the case for the commercial alloys, which normally contain both Ga and Pb as trace elements, by a similar mechanism [39].

Conclusions

- Presence of both Ga and Pb, of order 1000 and 10 ppm, respectively, can cause a significant increase in anodic activation of Al above that of the binary AlGa and AlPb alloys.
- Decreasing amount of Ga causes decrease in the degree of activation, while the amount of Pb has a minor effect.
- Heat-treatment temperature has a complex effect, determined by the nature of Pb segregation/enrichment near the metal surface.
- The mechanism of sustained activation by Pb and Ga is based on the following steps:
  - Pb segregation in the form of a continuous film and discrete particles, of order nanometre thickness, by heat treatment at the oxide-metal interface, causes the initial

activation when the ternary alloy AlGaPb is brought in contact with chloride environment.

  - Selective corrosion in areas activated by Pb segregation causes enrichment of Ga, probably in the form of a liquid AlGaPb phase.
  - The liquid phase destabilises the oxide further and causes increased activation and corrosion of Al through the phase.
  - The above steps cause an autocatalytic activation by increased dealloying and spreading of the Ga-rich amalgam over the alloy surface.
- At lower Ga concentrations and low heat-treatment temperatures, maintenance of the amalgam becomes unsustainable due to limited Pb and Ga segregation by heat treatment and dealloying, respectively.
- The above conclusions are limited to model AlGaPb alloys based on pure components.

Acknowledgements

This work was supported by The Research Council of Norway and Hydro Aluminium through the national research project Sustainable Aluminium Surface Applications (SALSA).

References

1. T. Furu, N. Telioui, C. Behrens, J. Hasenclever, P. Schaffer, Proceedings of the 12th International Conference on Aluminium Alloys (ICAA), 2010, Yokohama, Japan (2010), pp. 282-289.
2. A. J. Downs (Ed.), Chemistry of Aluminum, Gallium, Indium and Thallium, Chapman and Hall, London (1993).

3. L. E. Mordberg, Chem. Geol. 107 (1993) 241-244.
4. J. T. B. Gundersen, A. Aytaç, J. H. Nordlien, K. Nisancioglu, Corr. Sci. 46 (2004) 697-714.
5. Ø. Sævik, Y. Yu, J. H. Nordlien, K. Nisancioglu, J. Electrochem. Soc. 152 (2005) B334-B341.
6. J. C. Walmsley, Ø. Sævik, B. Graver, R. H. Mathiesen, Y. Yu, K. Nisancioglu, J. Electrochem. Soc. 154 (2007) C28-C35.
7. Anawati, B. Graver, H. Nordmark, Z. Zhao, G.S. Frankel, J.C. Walmsley, K. Nisancioglu, J. Electrochem. Soc. 157 (2010) C313-C320.
8. Z. Jia, B. Graver, J.C. Walmsley, Y. Yu, J.K. Solberg, K. Nisancioglu, J.Electrochem. Soc. 155 (2008) C1-C7.
9. Anawati, S. Diplas, K. Nisancioglu, J. Electrochem. Soc. 158 (2011) C158-C163.
10. Y. Yu, Ø. Sævik, J. H. Nordlien, K. Nisancioglu, J. Electrochem. Soc. 152 (2005) B327-B333.
11. Y. W. Keuong, J. H. Nordlien, K. Nisancioglu, J. Electrochem. Soc. 148 (2001) B497-B503.
12. A. Afseth, J. H. Nordlien, G. M. Scamans, K. Nisancioglu, Corr. Sci. 44 (2002)145-162.
13. A. R. Despic, D. M. Drazic, M. M. Purenovic, N. J. Cikovic, J. Appl. Electrochem. 6 (1976) 527-542.
14. C. D. S. Tuck, J. A. Hunter, G. M. Scamans, Electrochem. Sci. Tech. 134 (1987) 2970-2981.
15. C. B. Breslin, W. M. Carroll, Corr. Sci. 33 (1992) 1735-1746.
16. Y. W. Keuong, J. H. Nordlien, S. Ono, K. Nisancioglu, J. Electrochem. Soc. 150 (2003) B547-B551.

17. B. Graver, A. T. J. van Helvoort, K. Nisancioglu, Corr. Sci. 52 (2010) 3774-3781.

18. B. Graver, A. M. Pedersen and K. Nisancioglu, ECS Trans., 16(52) (2009) 55-69.

19. J. Tan, K. Nisancioglu, Corr. Sci., 76 (2013) 219–230.

20. Anawati, M. P. Halvorsen, K. Nisancioglu, J. Electrochem. Soc., 159 (2012) C211-C218.

21. E. Senel, K. Nisancioglu, Corr. Sci., 85 (2014) 436–444.

22. J. T. Reding, J. J. Newport, Mater. Prot., 5(12) (1966)15-18.

23. I. N. Gantsev, M. H. Shukroev, J. Appl. Chem. USSR (USA) 64 (1991) 50-53.

24. B. Graver, A. T. J. van Helvoort, J. C. Walmsley, K. Nisancioglu, Mater. Sci. Forum, 519-521 (2006) 673-678.

25. K. Fukuoka, Sumitomo Light Metal Technical Reports, 42 (2001) 131.

26. M. R. Pinnel, J. E. Bennett, J. Mater. Sci., 7 (1972) 1016-1026.

27. J. B. Bessone, Corr. Sci., 48 (2006) 4243-4256.

28. D. O. Flamini, L. Cunci, S. B. Saidman, Mater. Chem. & Phys., 108 (2008) 33–38.

29. D. O. Flamini, S. B. Saidman, J. B Bessone, Corr. Sci., 48 (2006) 1413–1425.

30. G. L. Allen, R. A. Bayles, W. W. Gile, W. A. Jesser, Thin Solid Films, 144 (1986) 297.

31. C. J. Coombes, J. Phys. F, 2 (1972) 441.

32. Y. Lereah, G. Deutscher, P. Cheyssac, R. Kofman, Europhys. Lett., 12 (1990) 709.

33. K. Kurt, S. Diplas, J. C. Walmsley, K. Nisancioglu, J. Electrochem. Soc., 160 (2013) C542-C552.

34. E. Senel, K. Nisancioglu, Corr. Sci., 88 (2014) 280-290.

35. Certified Reference Materials, Swerea/Kimab, Kista, Sweden, http://www.swerea.se/en/services/analyses-testing-studies/certified-reference-materials-crm (2015).

36. E. Senel, J. C. Walmsley, S. Diplas, K. Nisancioglu, Corr. Sci., 85 (2014) 167–173.
37. Anawati, S. Diplas, B. Holme, J. K. Solberg, R. H. Mathiesen, J. C. Walmsley, K. Nisancioglu, J. Electrochem. Soc., 158 (2011) C178-C184.
38. K. Shimizu, R.C. Furneaux, G.E. Thompson, G.C. Wood, A. Gotoh, K. Kobayashi, Oxid. Met., 35 (1991) 427-439.
39. E. Senel, PhD Thesis, Norwegian University of Science and Technology, Trondheim, Norway (2012).
40. S. Aloni, M. Polak, Surf. Sci. (1996) L123-L127.
41. M. Allione, R. Kofman, F. Celestini, Y. Lereah, Eur. Phys. J. D, 52 (2009) 207-210.

Figure Captions

Figure 1. GD-OES elemental depth profiles for alloys a) AlGa50Pb50 and b) AlGa1000Pb50 after heat treatment for 1 h at 450°C and c) for alloy AlGa1000Pb50 after heat treatment at 600°C. All heat-treated samples were quenched in water after heat treatment.

Figure 2. Potentiodynamic polarization curves for samples in conditions a) as-polished and heat-treated for 1 h at b) 300°C, c) 450°C and 600°C. The curves without the temperature label in (c) were heat-treated at 600°C.

Figure 3. Corrosion potentials of alloys AlGa1000Pb50 and AlGa1000 in acidified synthetic seawater. Both alloys were heat-treated for 1 h at 600°C.

Figure 4. Potentiostatic polarization results a) for alloy AlGa50Pb50 at an applied potential of -0.8 V_{SCE} and for alloy AlGa1000Pb50 at potentials b) -0.8 V_{SCE} and c) -0.9 V_{SCE} after heat treatment at different temperatures. Fig. 4b includes the curves for an as-polished sample (not heat-treated) and an AlGa1000 sample (heat-treated at 300°C) polarized at -0.8 V_{SCE}, as reference.

Figure 5. Potentiostatic polarization results for samples heat-treated at 600°C at applied potentials of a) -0.93 V_{SCE} and b) -0.88 V_{SCE}.

Figure 6. Surface morphology of alloy AlGa1000Pb50 (annealed at 600°C) after potentiodynamic polarization to -0.93 $V_{SCE,}$ investigated *ex-situ* by SEM. a) General view of the corroded area marked A for uncorroded areas and B for corroded areas. b) Undermined

oxide at higher magnification of area marked in (a). c), d) Propagation of corrosion at corresponding areas marked in (a). e) Back-scattered electron image of (d) where bright spots are Pb particles.

Figure 7. Surface morphology of alloy AlGa1000Pb50 (annealed at 600°C) after potentiodynamic polarization to -0.92 V_{SCE}, investigated by ex-situ SEM.

Figure 8. Surface morphology after potentiostatic polarisation of alloy AlGa1000Pb50 (annealed at 300°C) for 2 h at -0.9 V_{SCE}. a) General appearance of the corroded area. b) Marked area in (a) at a higher magnification. c) Marked area in (b) at a higher magnification and EDS analysis of the spot marked X.

Figure 9. GD-OES analysis of alloy AlGa1000Pb50 (annealed for 1 h at 600°C) after polarising for 10 min at a) -0.93 V_{SCE} and b) -0.88 V_{SCE}. c) GD-OES analysis after polarising alloy AlGa1000Pb50 (annealed for 1 h at 300°C) for 10 min at -0.8 V_{SCE}.

Figure 10. Comparison of Ga and Pb enrichment on alloy AlGa1000Pb50 after annealing at different temperatures (annealed), calculated by integration of the GD-OES data, and after potentiostatic polarisation at -0.8 V_{SCE} (corroded), calculated by integration of the data in Fig. 4a and 5b for the first 10 min.

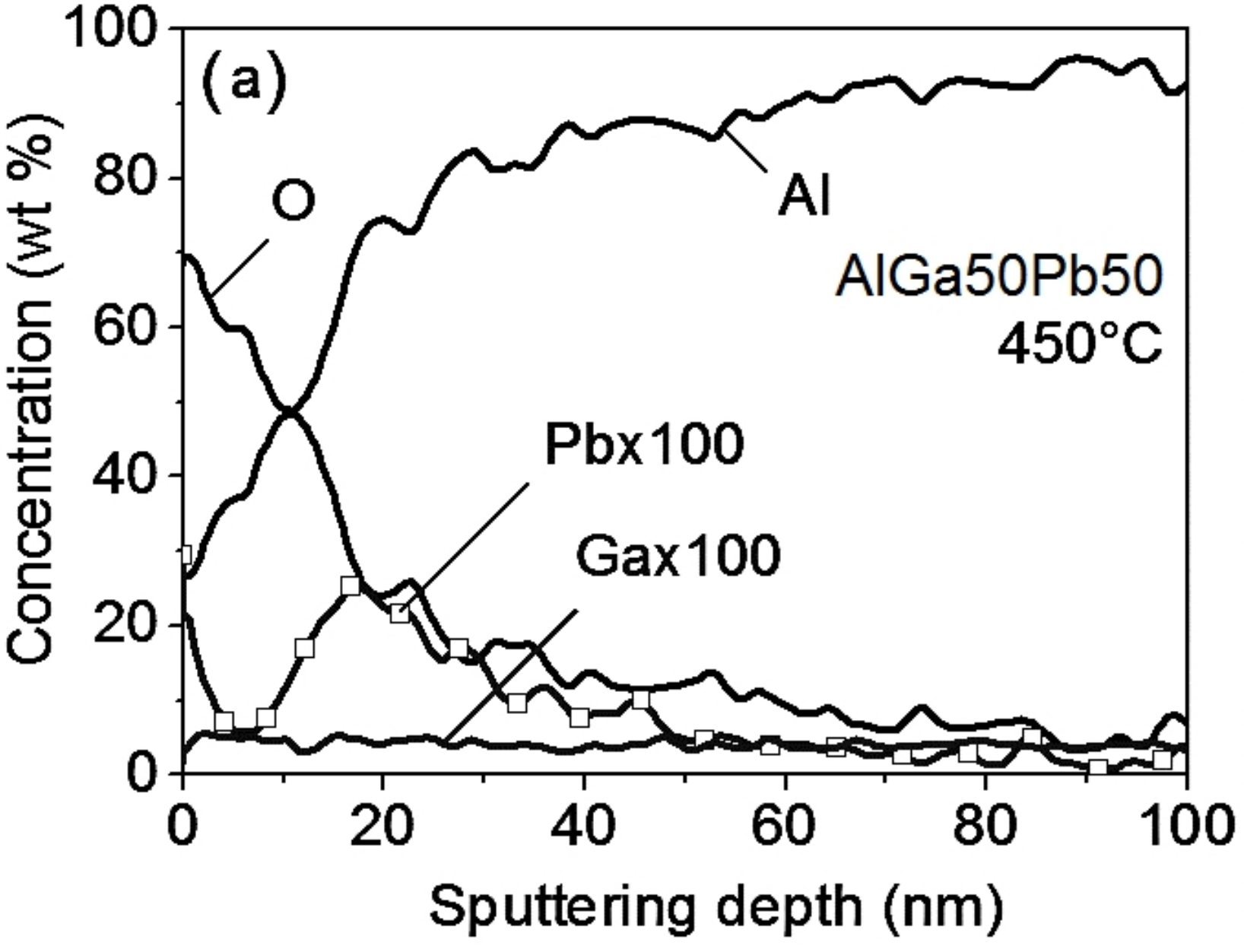
(a)
O
Al
AlGa50Pb50
450°C
Pbx100
Gax100
Concentration (wt %)
Sputtering depth (nm)
0
20
40
60
80
100

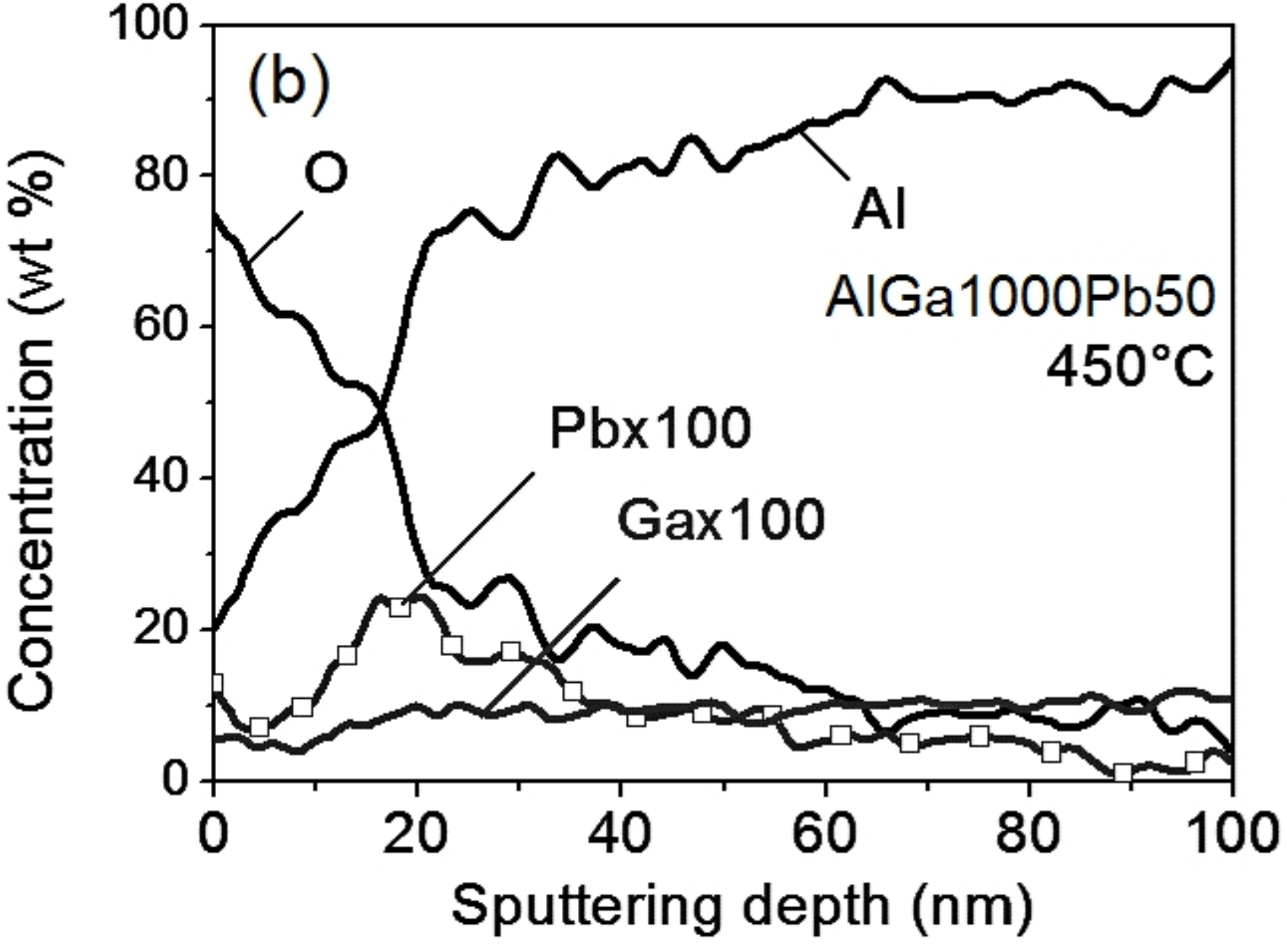
(b)
O
Al
AlGa1000Pb50
450°C
Pbx100
Gax100
Concentration (wt %)
Sputtering depth (nm)
0
20
40
60
80
100

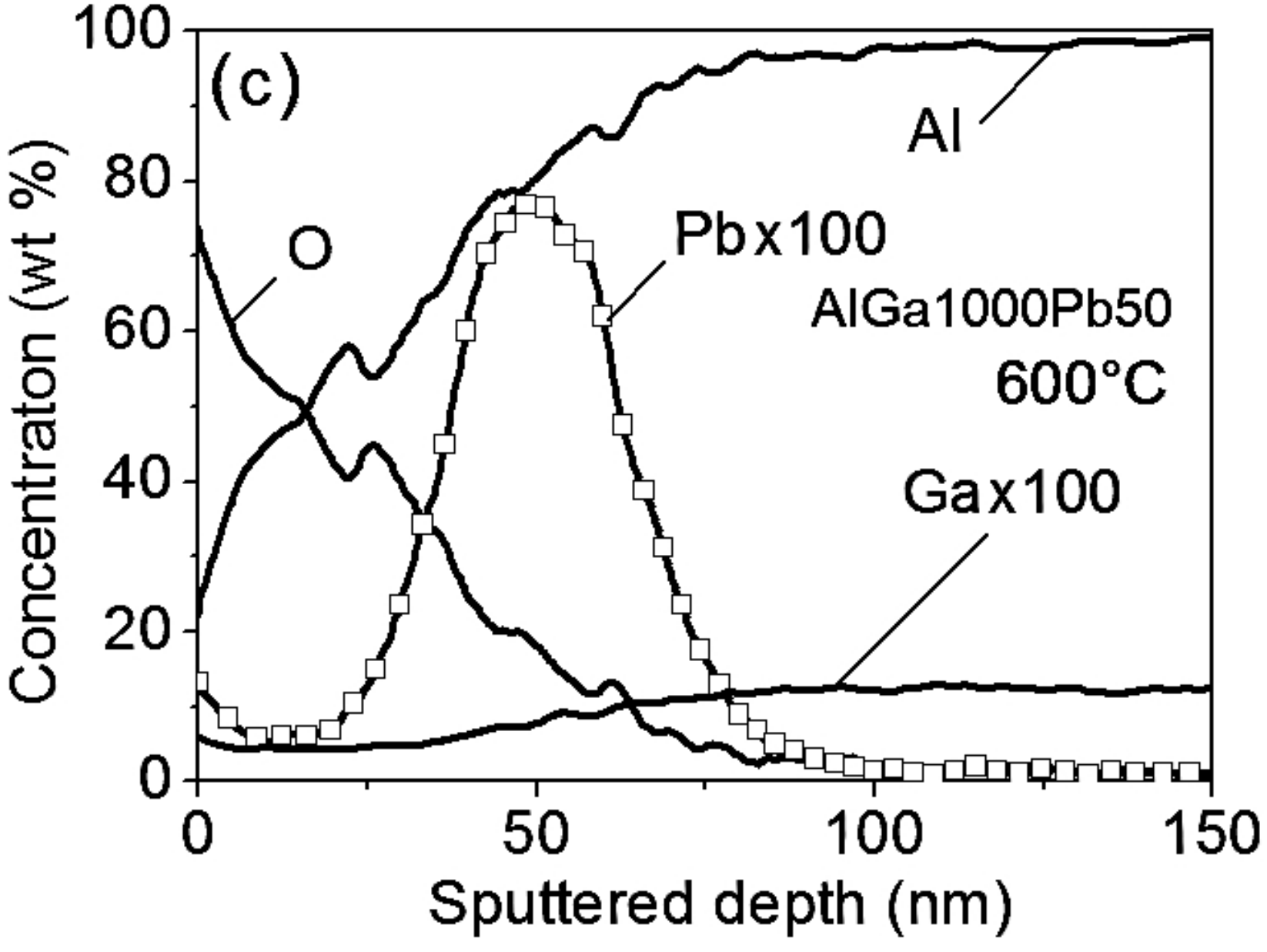
(c)
Al
O
Pbx100
AlGa1000Pb50
600°C
Gax100
Concentraton (wt %)
Sputtered depth (nm)
0
20
40
60
80
100
0
50
100
150

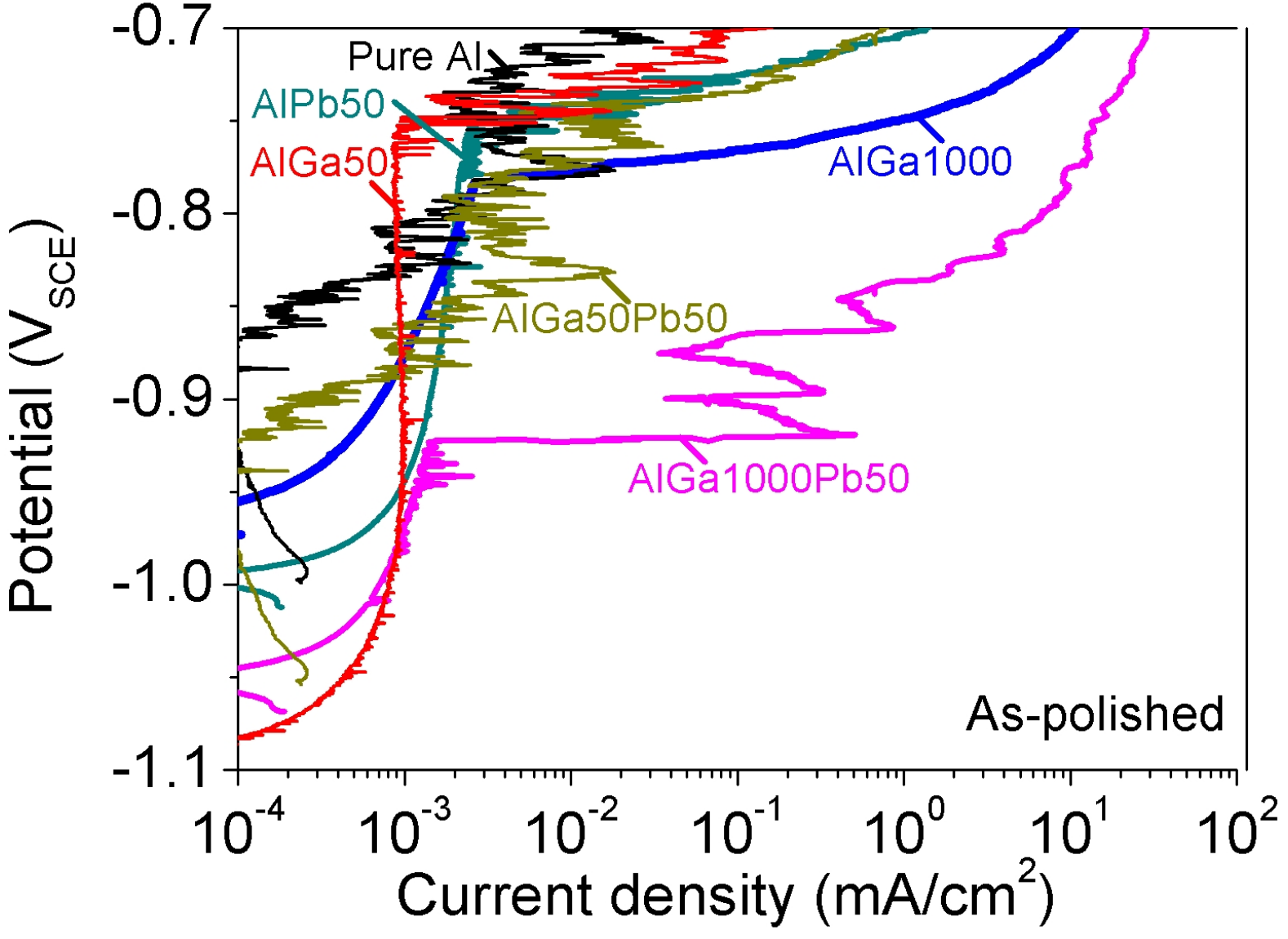
-0.7
-0.8
-0.9
-1.0
-1.1
Potential (V_{SCE})
Pure Al
AlPb50
AlGa50
AlGa1000
AlGa50Pb50
AlGa1000Pb50
As-polished
10^{-4}
10^{-3}
10^{-2}
10^{-1}
10^{0}
10^{1}
10^{2}
Current density (mA/cm^2)

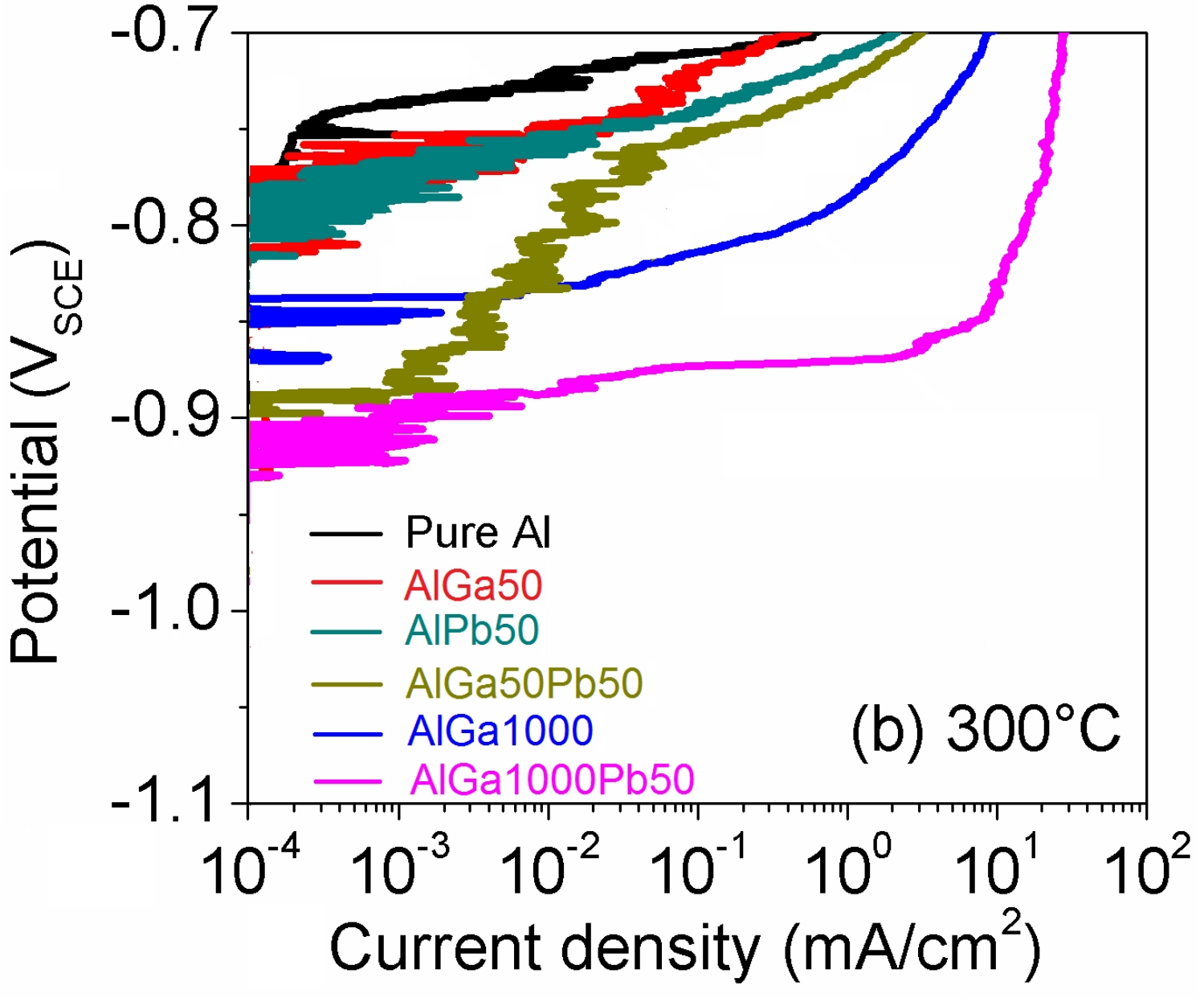
-0.7
-0.8
-0.9
-1.0
-1.1
Potential (V_{SCE})
Pure Al
AlGa50
AlPb50
AlGa50Pb50
AlGa1000
AlGa1000Pb50
(b) 300°C
10^{-4} 10^{-3} 10^{-2} 10^{-1} 10^{0} 10^{1} 10^{2}
Current density (mA/cm^2)

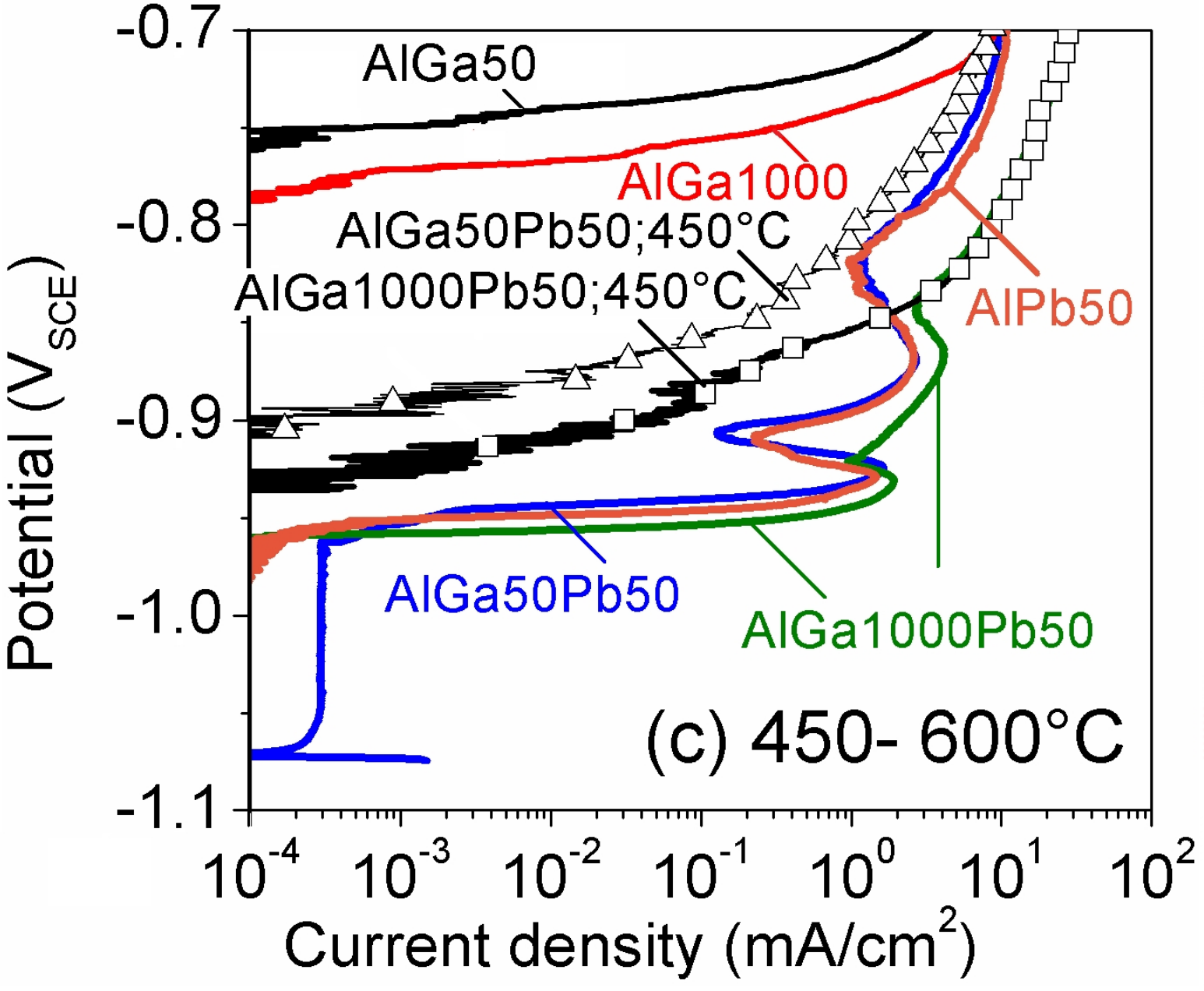
-0.7
-0.8
-0.9
-1.0
-1.1
Potential (V_{SCE})
AlGa50
AlGa1000
AlGa50Pb50;450°C
AlGa1000Pb50;450°C
AlPb50
AlGa50Pb50
AlGa1000Pb50
(c) 450- 600°C
10^{-4} 10^{-3} 10^{-2} 10^{-1} 10^{0} 10^{1} 10^{2}
Current density (mA/cm^2)

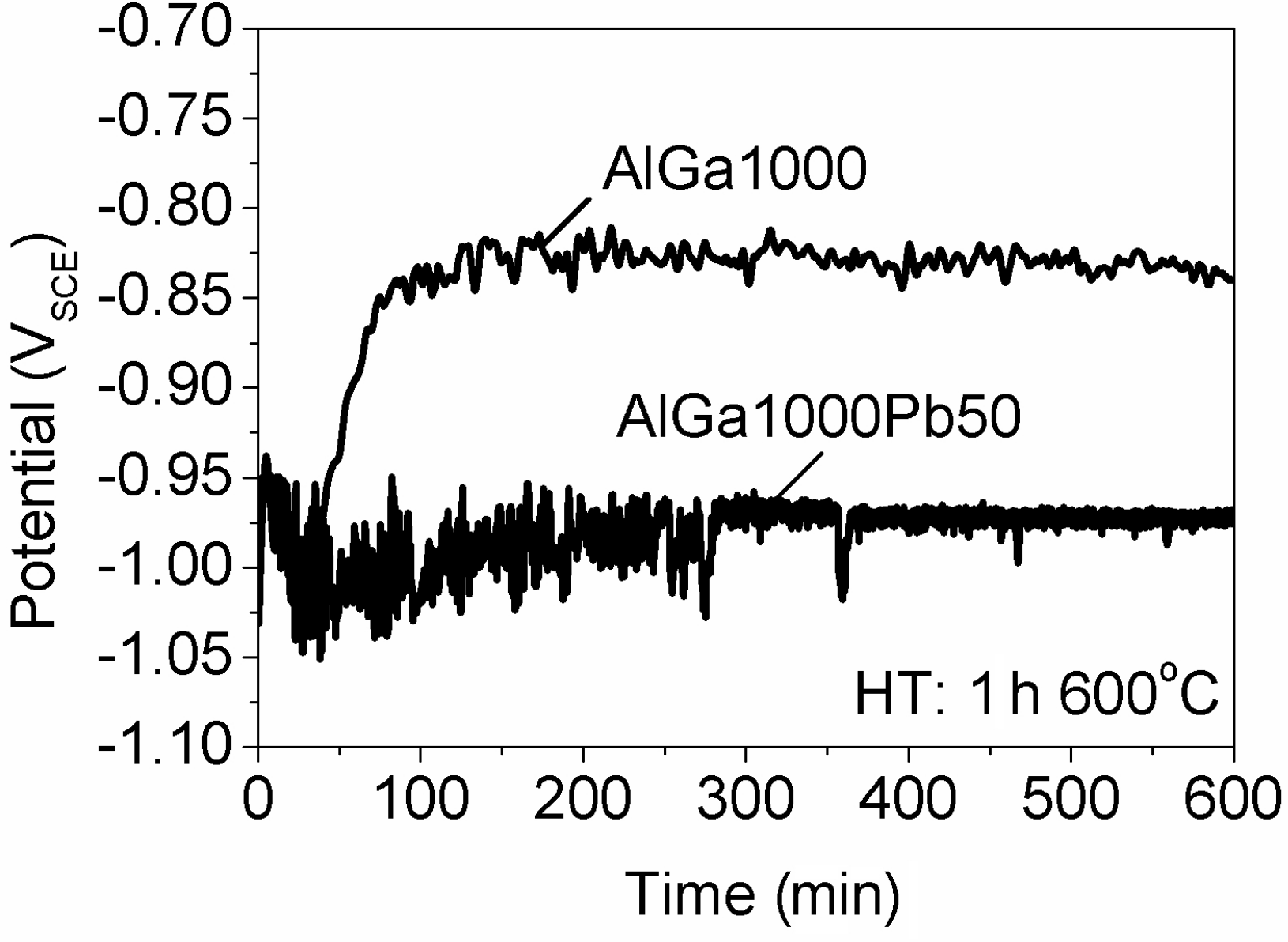
-0.70
-0.75
-0.80
-0.85
-0.90
-0.95
-1.00
-1.05
-1.10
Potential (V_{SCE})
AlGa1000
AlGa1000Pb50
HT: 1 h 600°C
0
100
200
300
400
500
600
Time (min)

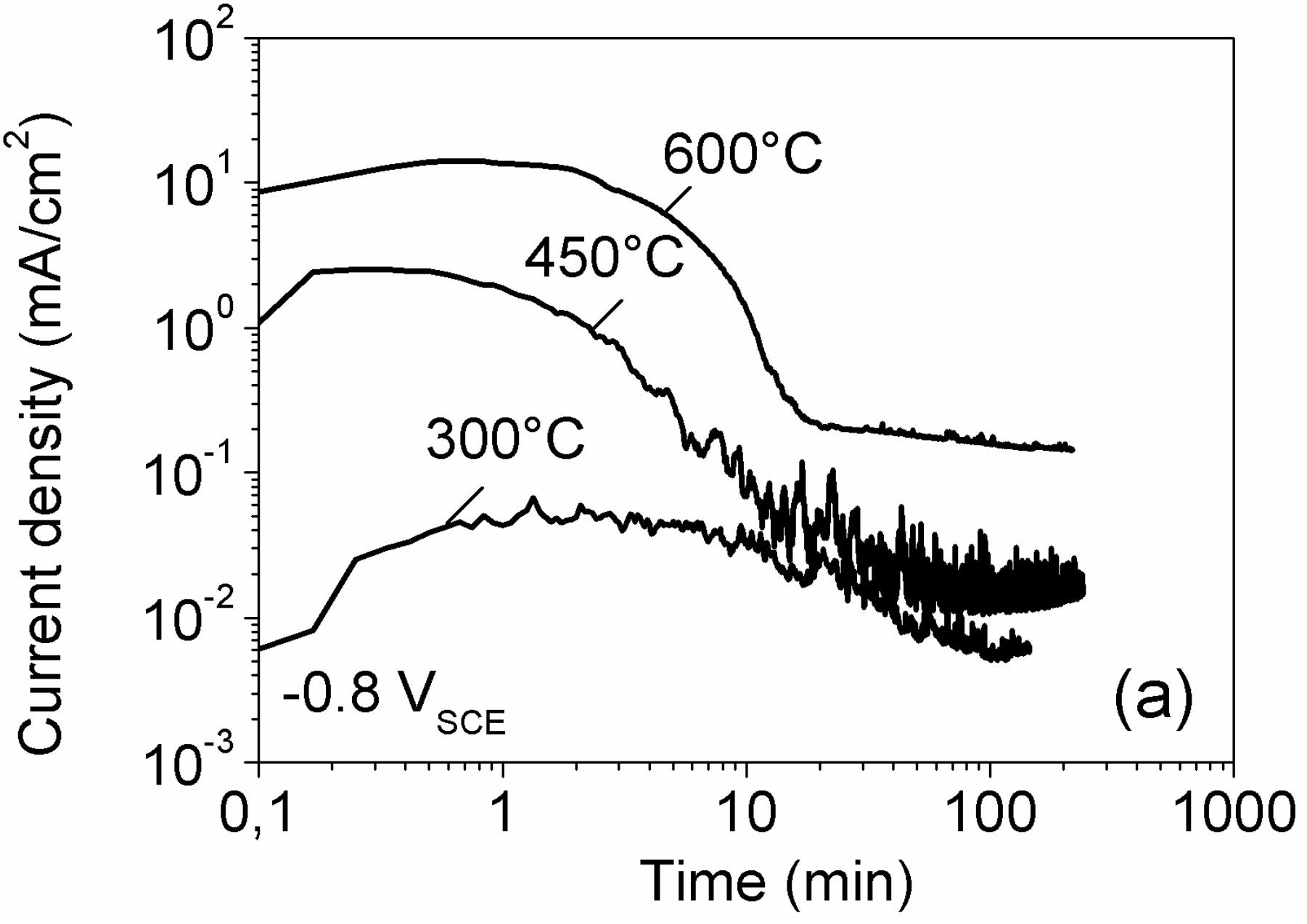
Current density (mA/cm^2)
10^2
10^1
10^0
10^{-1}
10^{-2}
10^{-3}
600°C
450°C
300°C
-0.8 V_{SCE}
(a)
0,1
1
10
100
1000
Time (min)

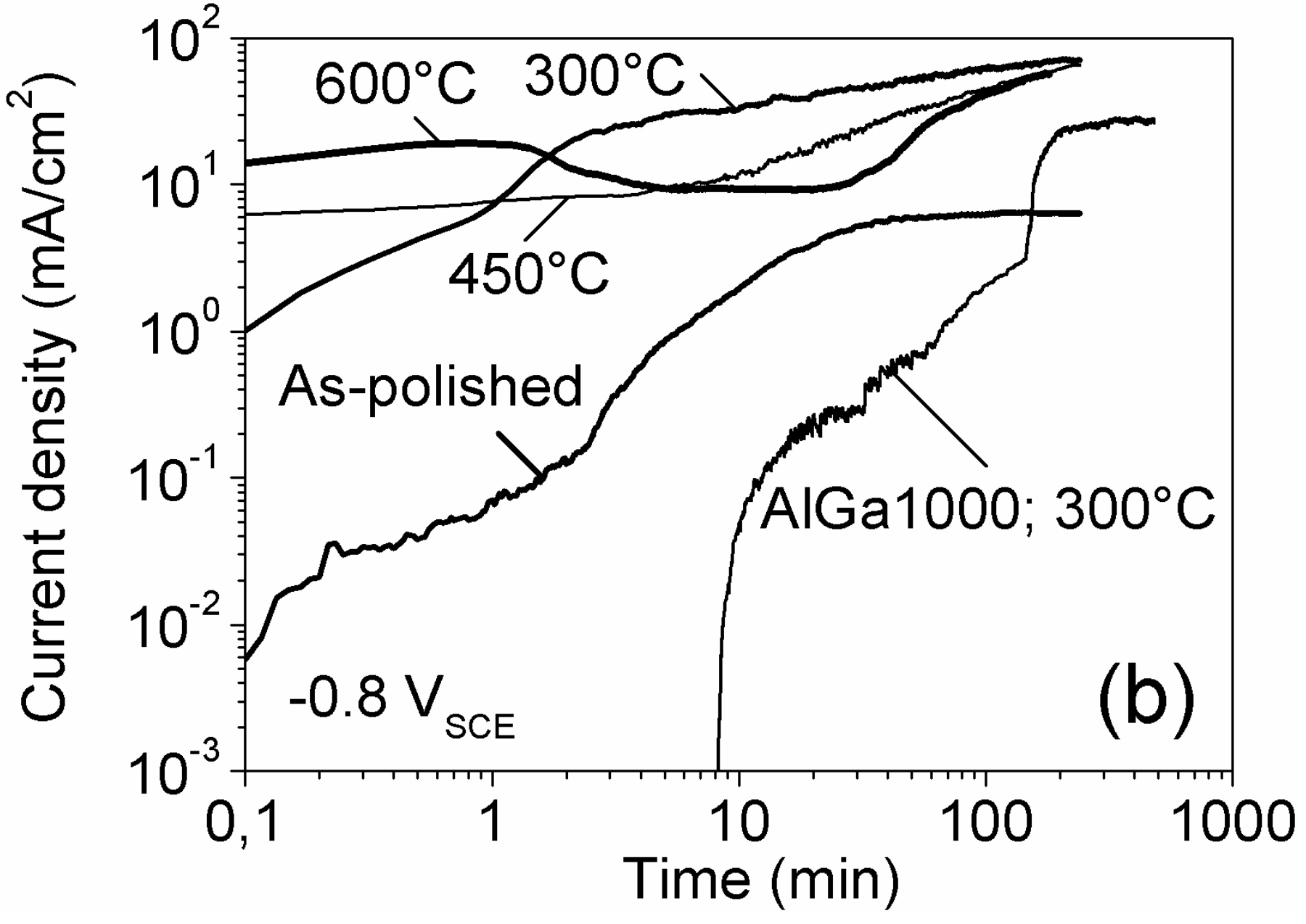
Current density (mA/cm^2)
10^2
10^1
10^0
10^{-1}
10^{-2}
10^{-3}
600°C
300°C
450°C
As-polished
AlGa1000; 300°C
-0.8 V_{SCE}
(b)
0,1
1
10
100
1000
Time (min)

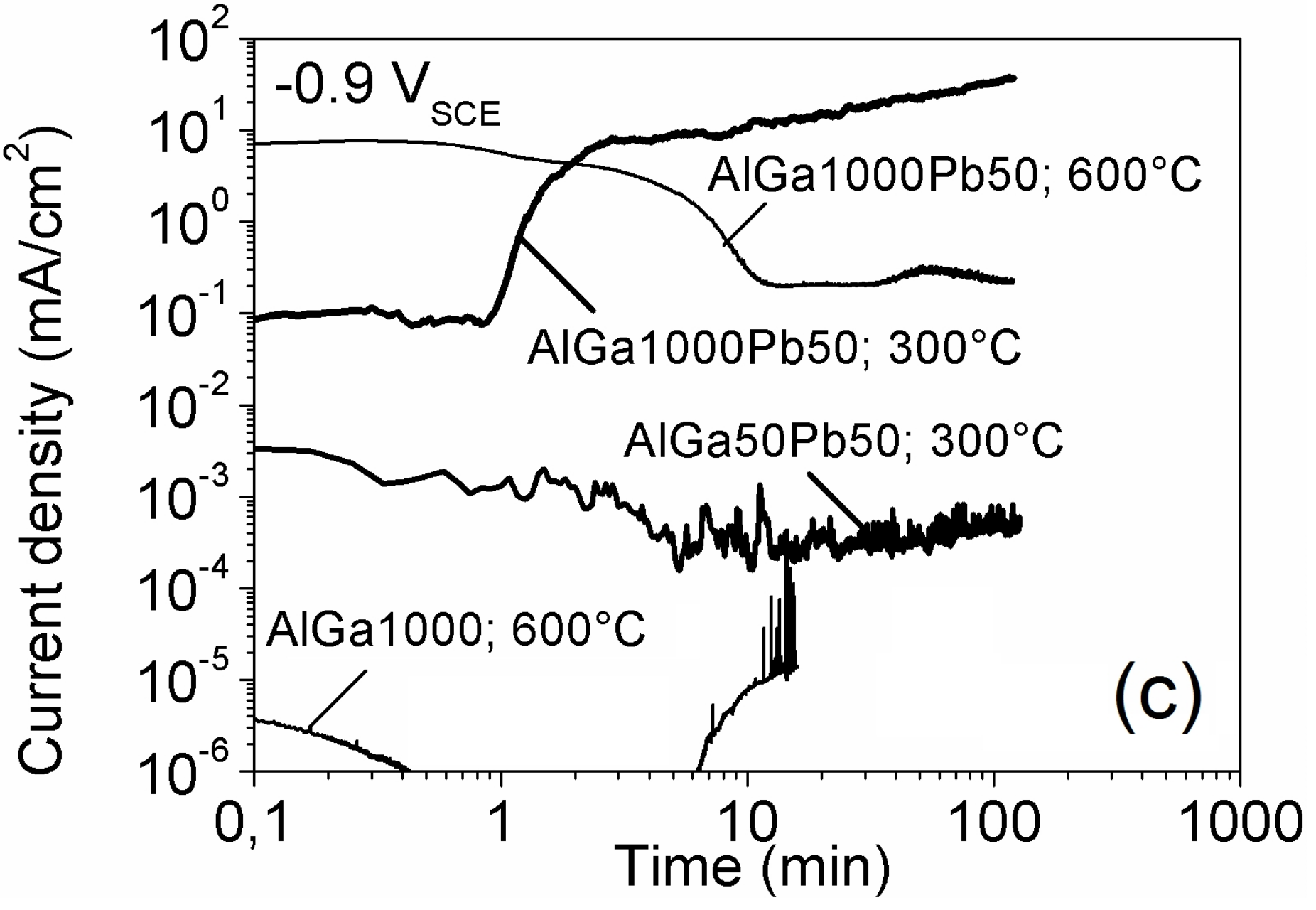
-0.9 V SCE
AlGa1000Pb50; 600°C
AlGa1000Pb50; 300°C
AlGa50Pb50; 300°C
AlGa1000; 600°C
(c)
Current density (mA/cm2)
Time (min)
10^2
10^1
10^0
10^-1
10^-2
10^-3
10^-4
10^-5
10^-6
0,1
1
10
100
1000

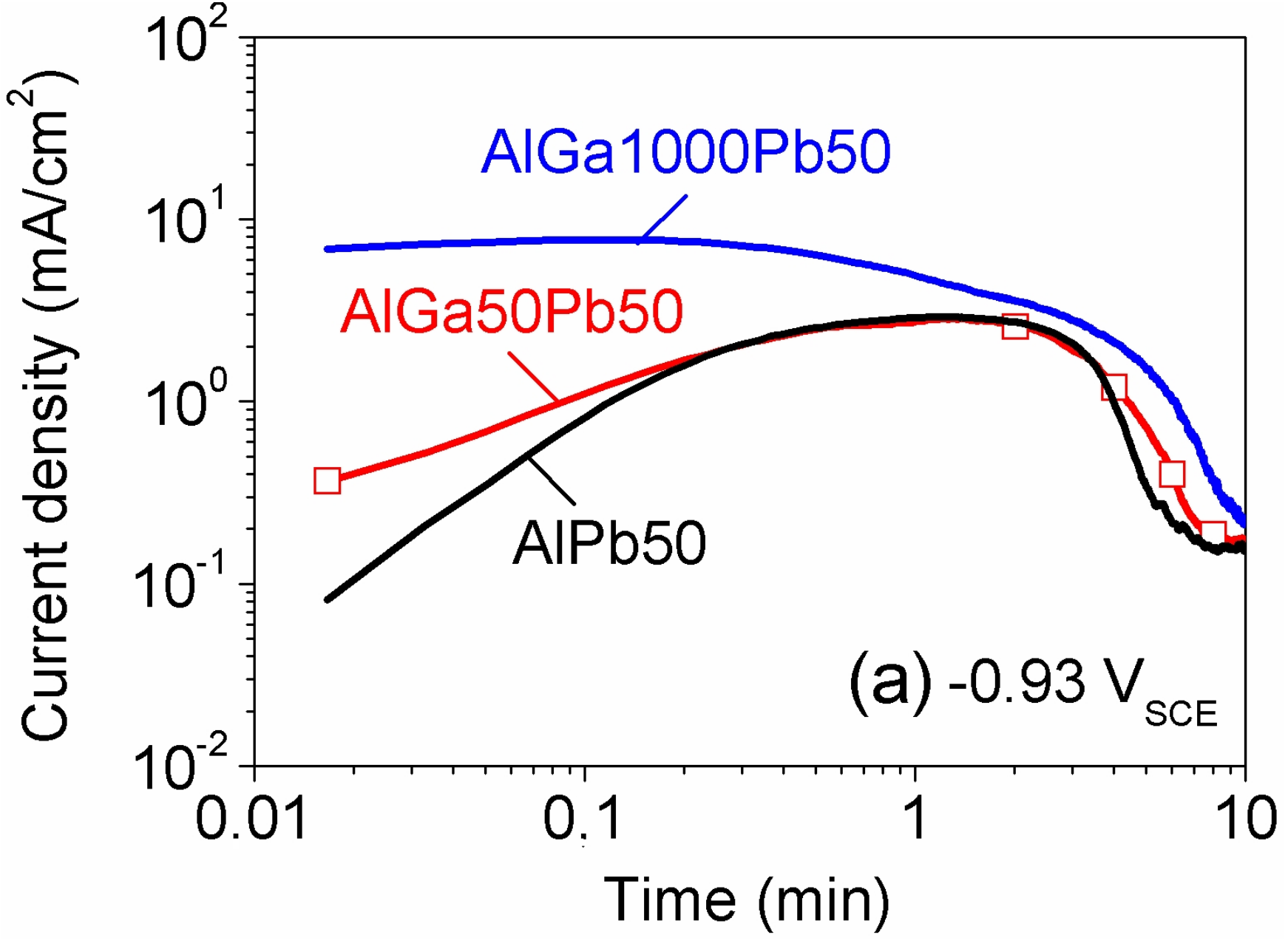
Current density (mA/cm^2)
10^2
10^1
10^0
10^{-1}
10^{-2}
0.01
0.1
1
10
Time (min)
AlGa1000Pb50
AlGa50Pb50
AlPb50
(a) -0.93 V_{SCE}

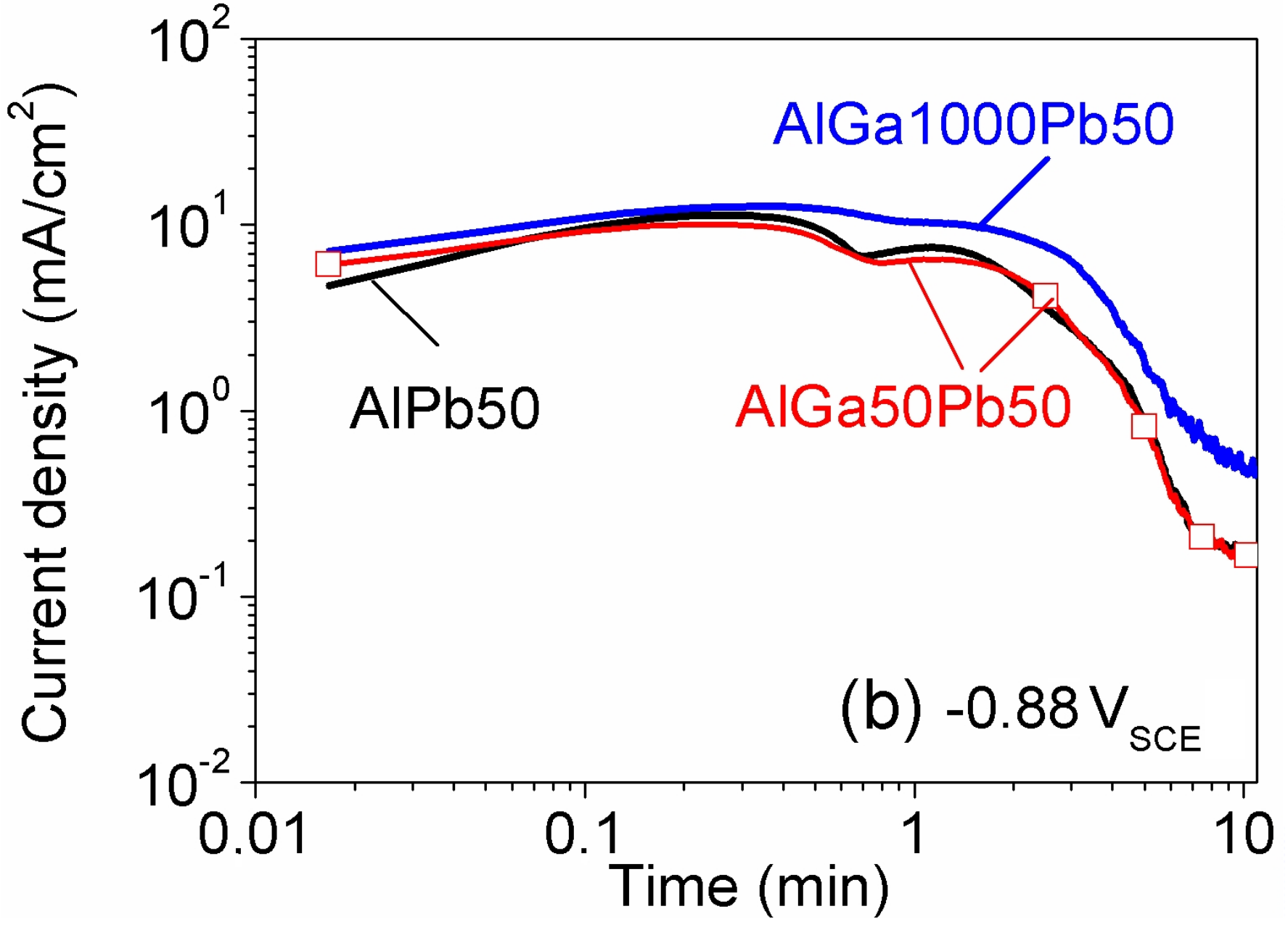
Current density (mA/cm^2)
10^2
10^1
10^0
10^{-1}
10^{-2}
0.01
0.1
1
10
Time (min)
AlGa1000Pb50
AlPb50
AlGa50Pb50
(b) -0.88 V_{SCE}

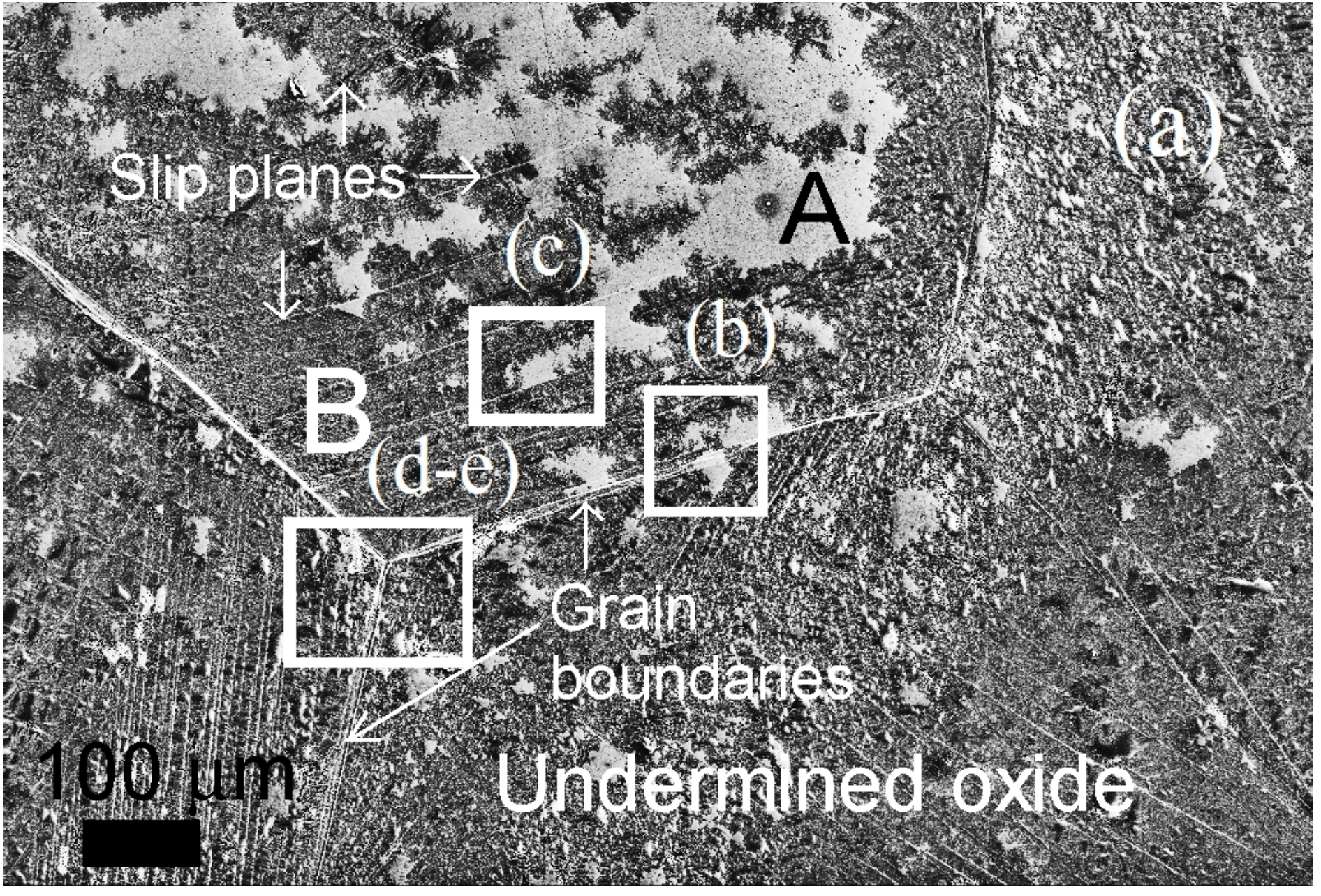
Slip planes
(a)
A
(c)
(b)
B
(d-e)
Grain
boundaries
100 µm
Undermined oxide

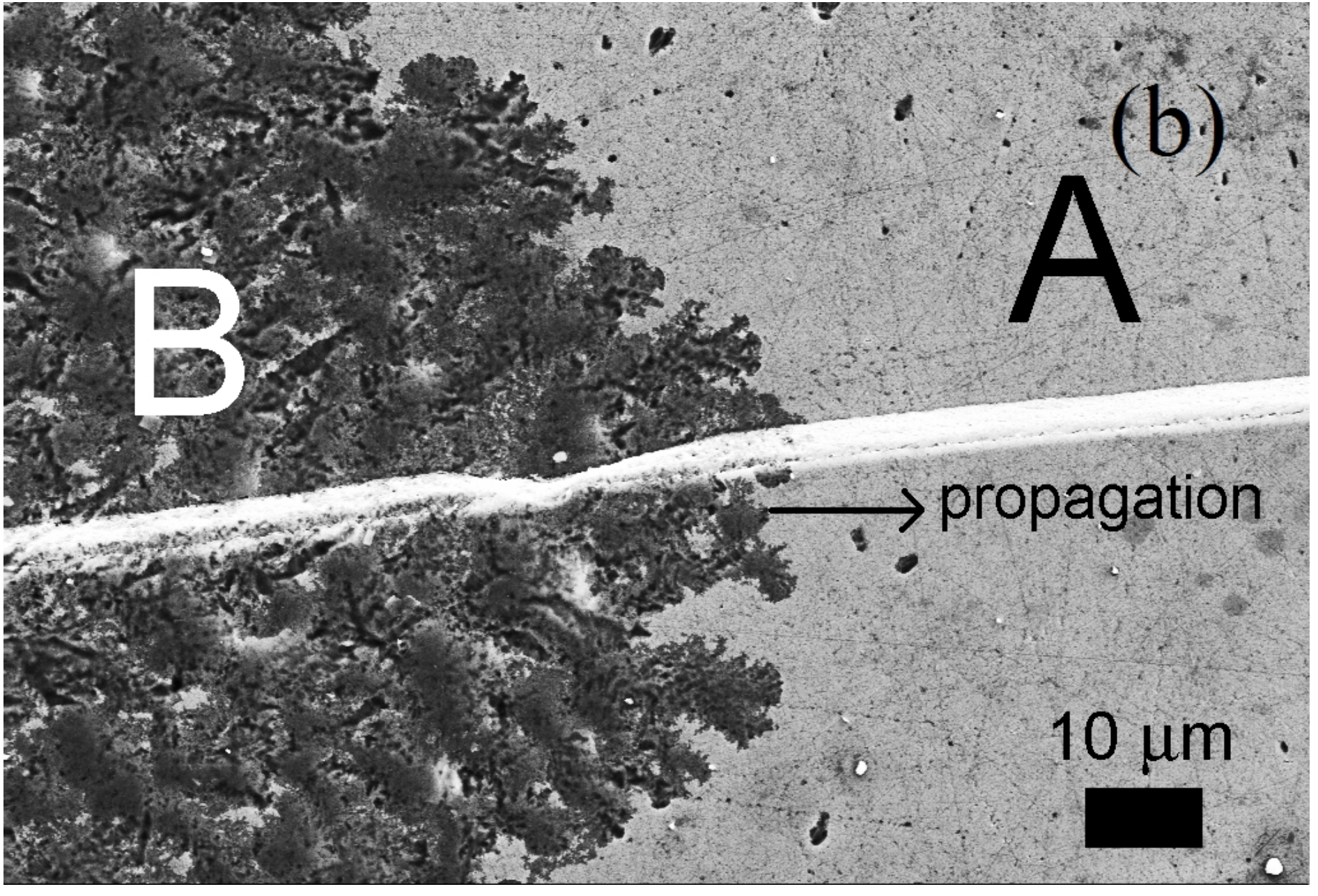
(b)
A
B
propagation
10 µm

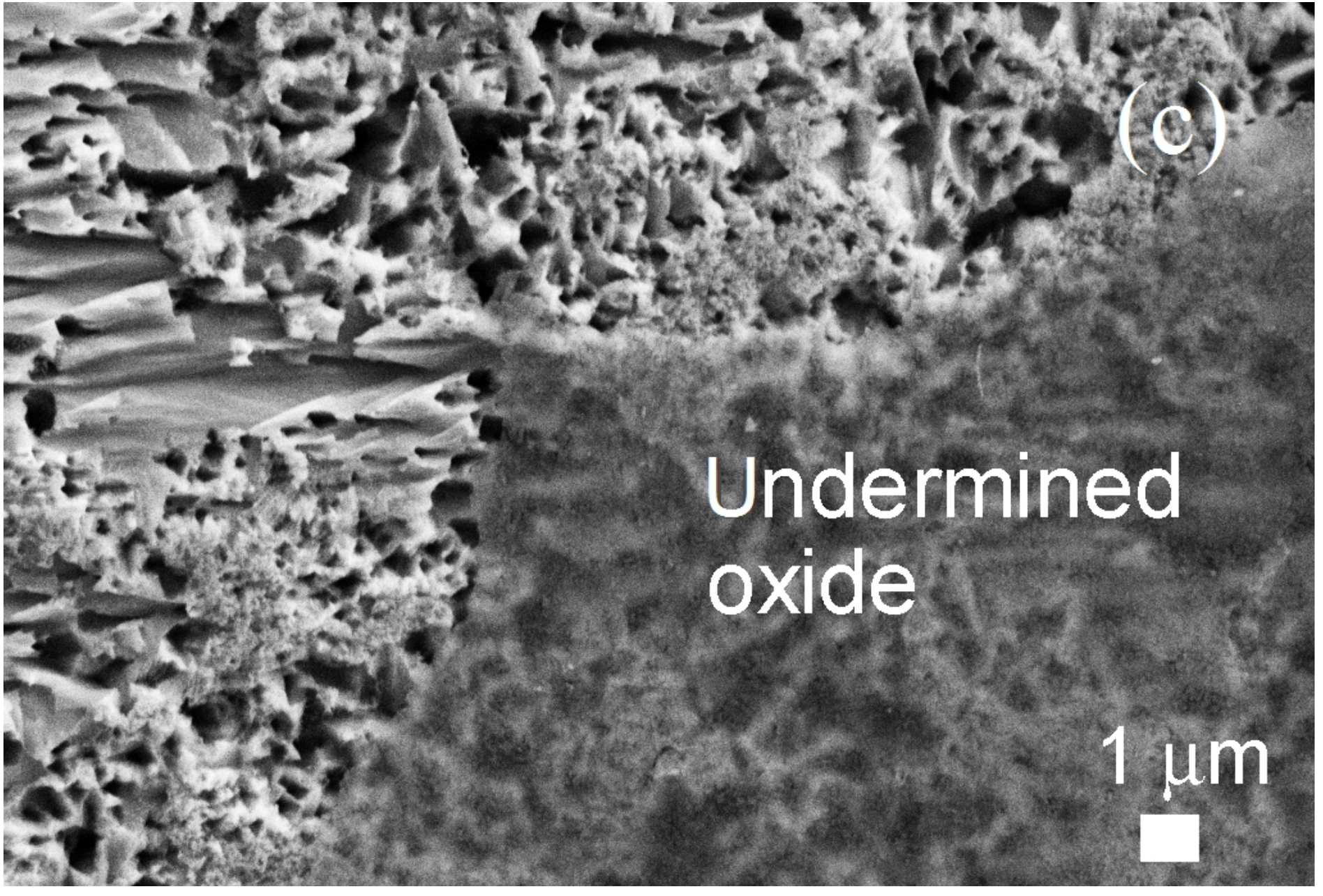
(c)
Undermined
oxide
1 μm

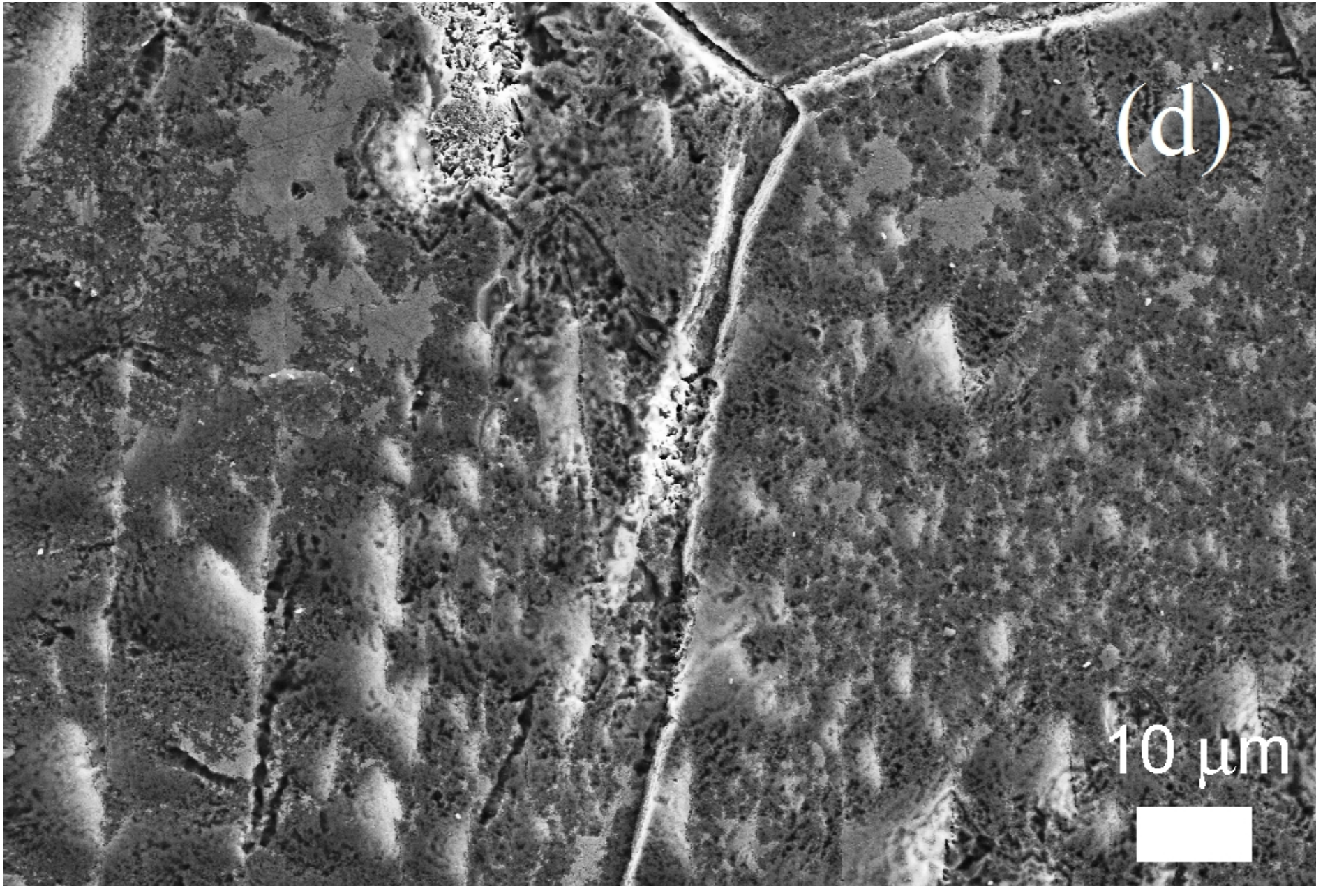
(d)
10 µm

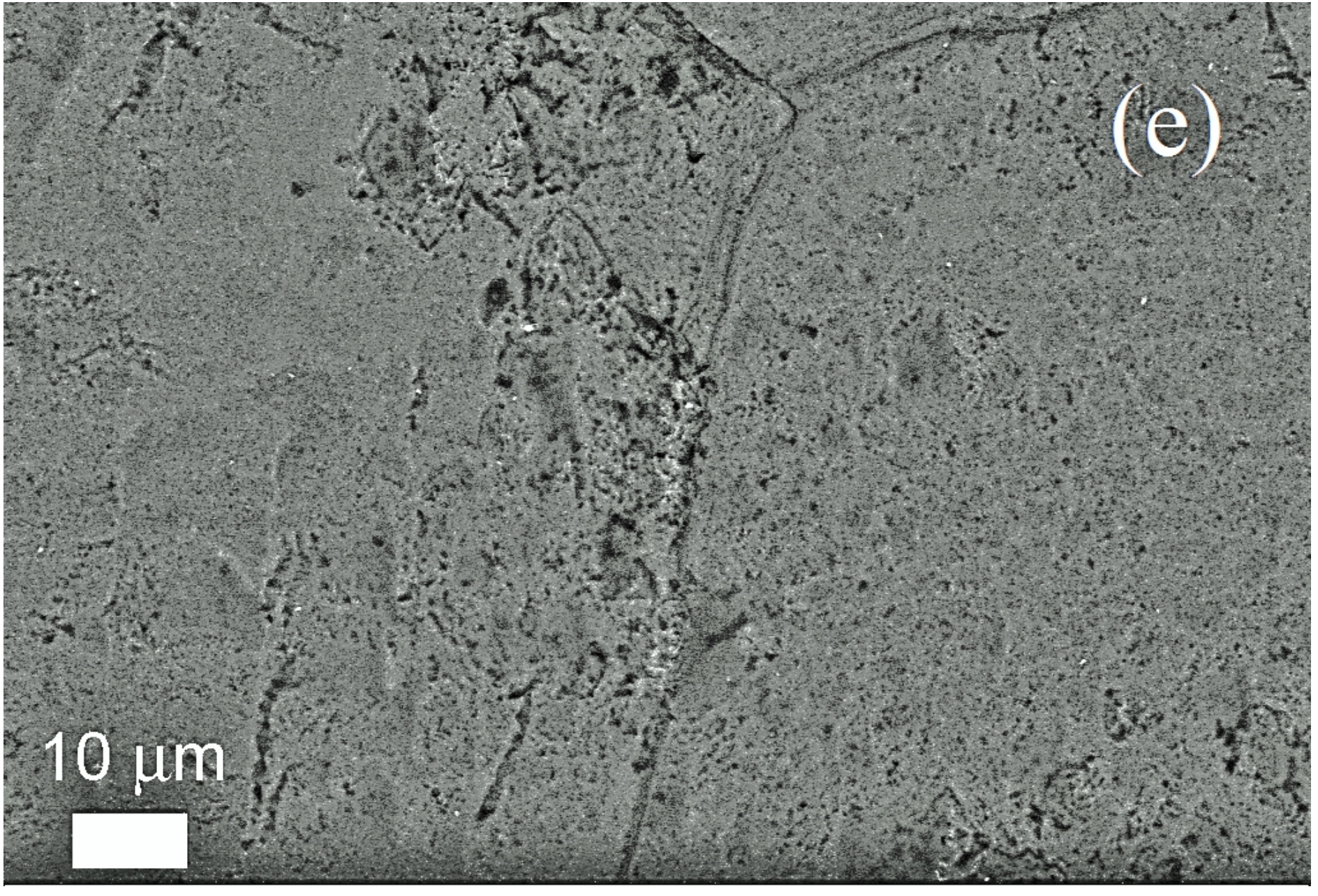
(e)
10 µm

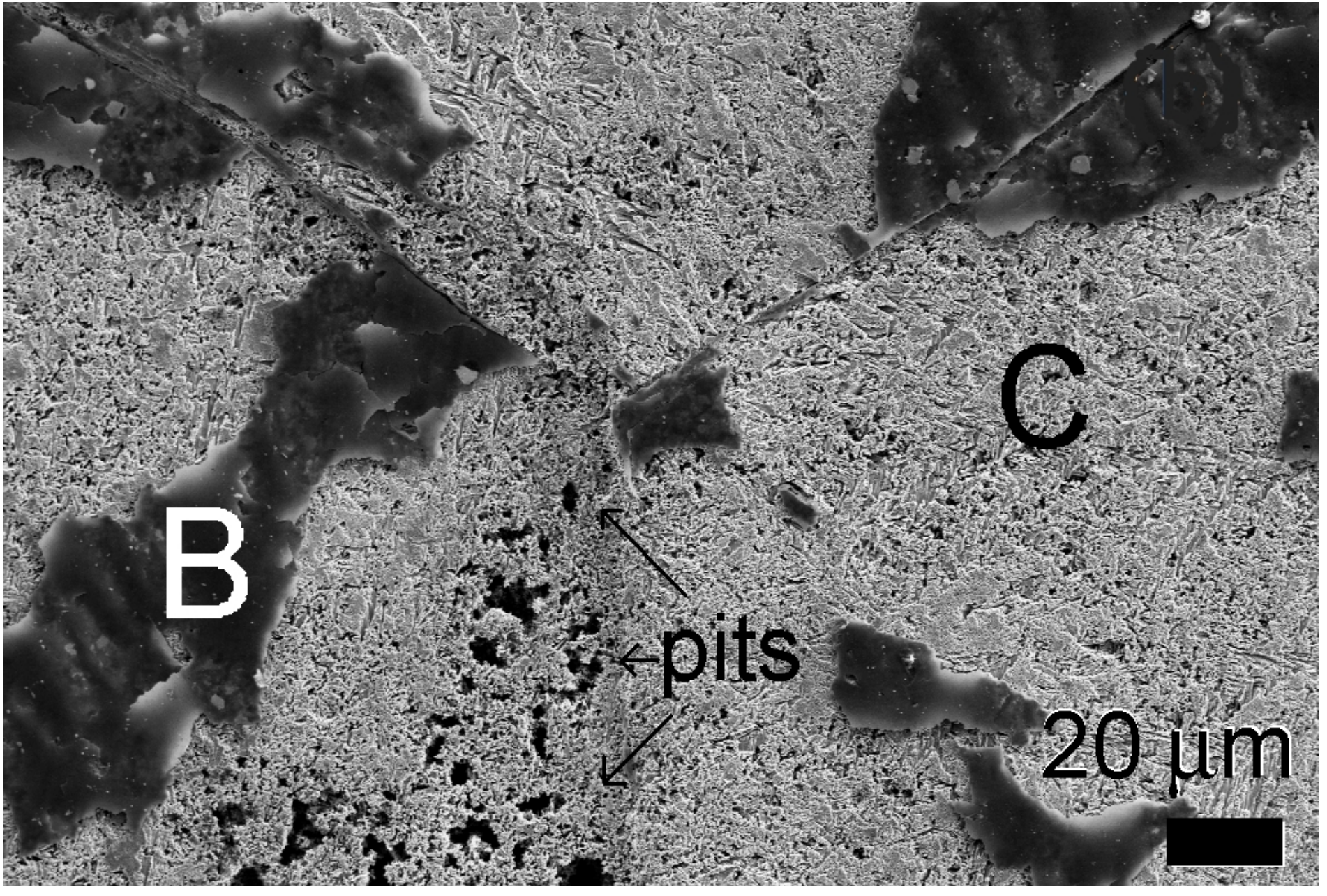
B
C
pits
20 µm

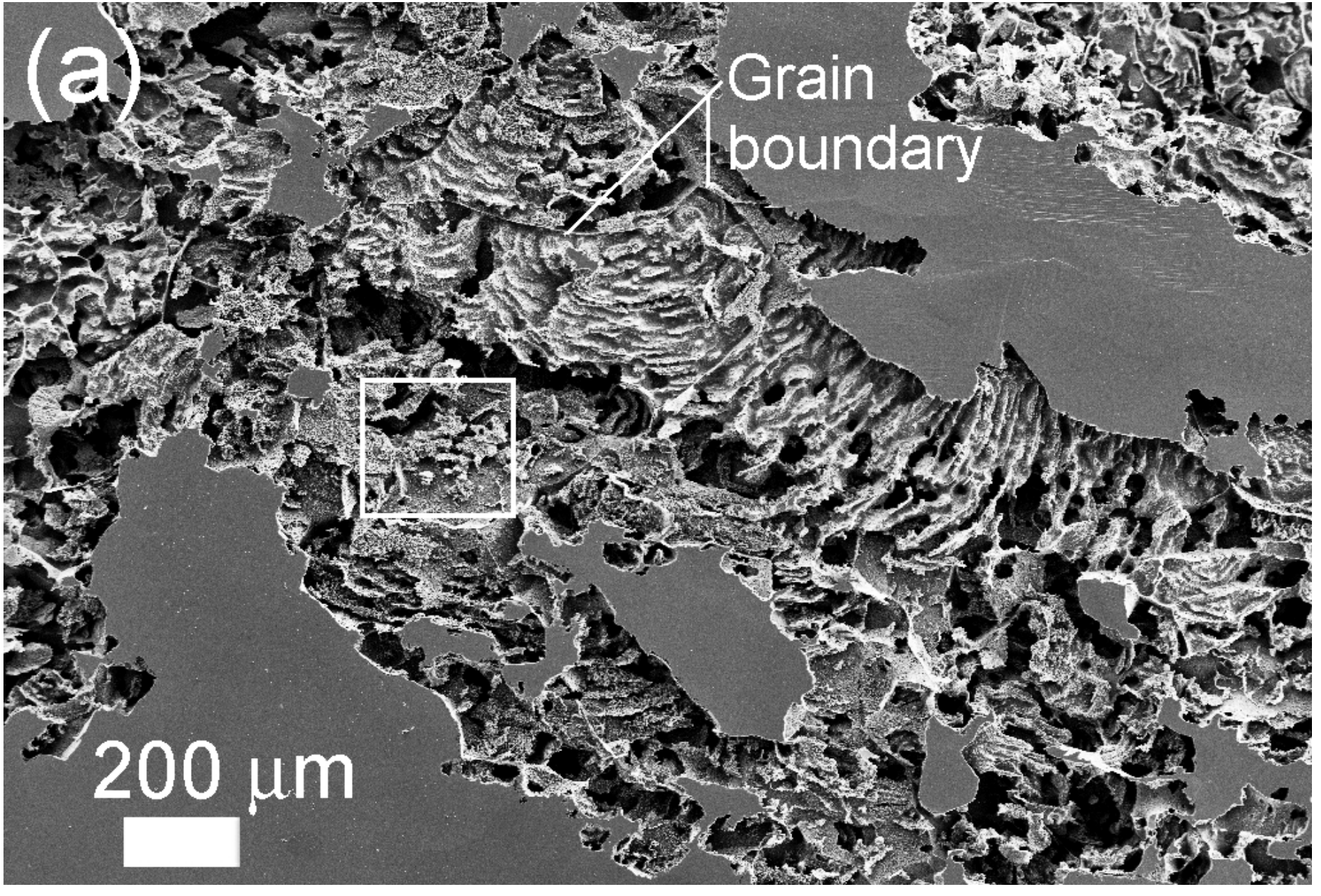
(a)
Grain
boundary
200 μm

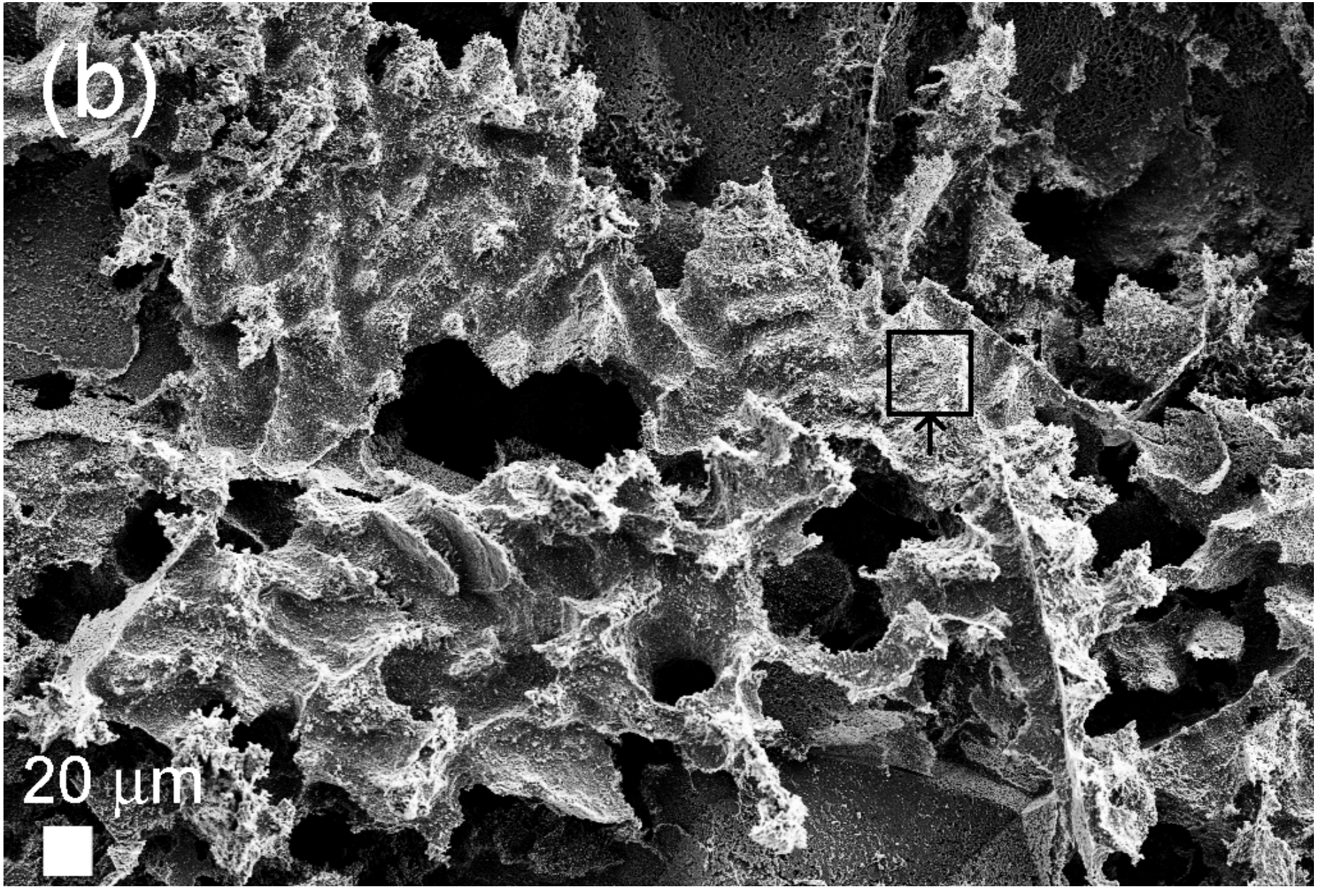
(b)
20 μm

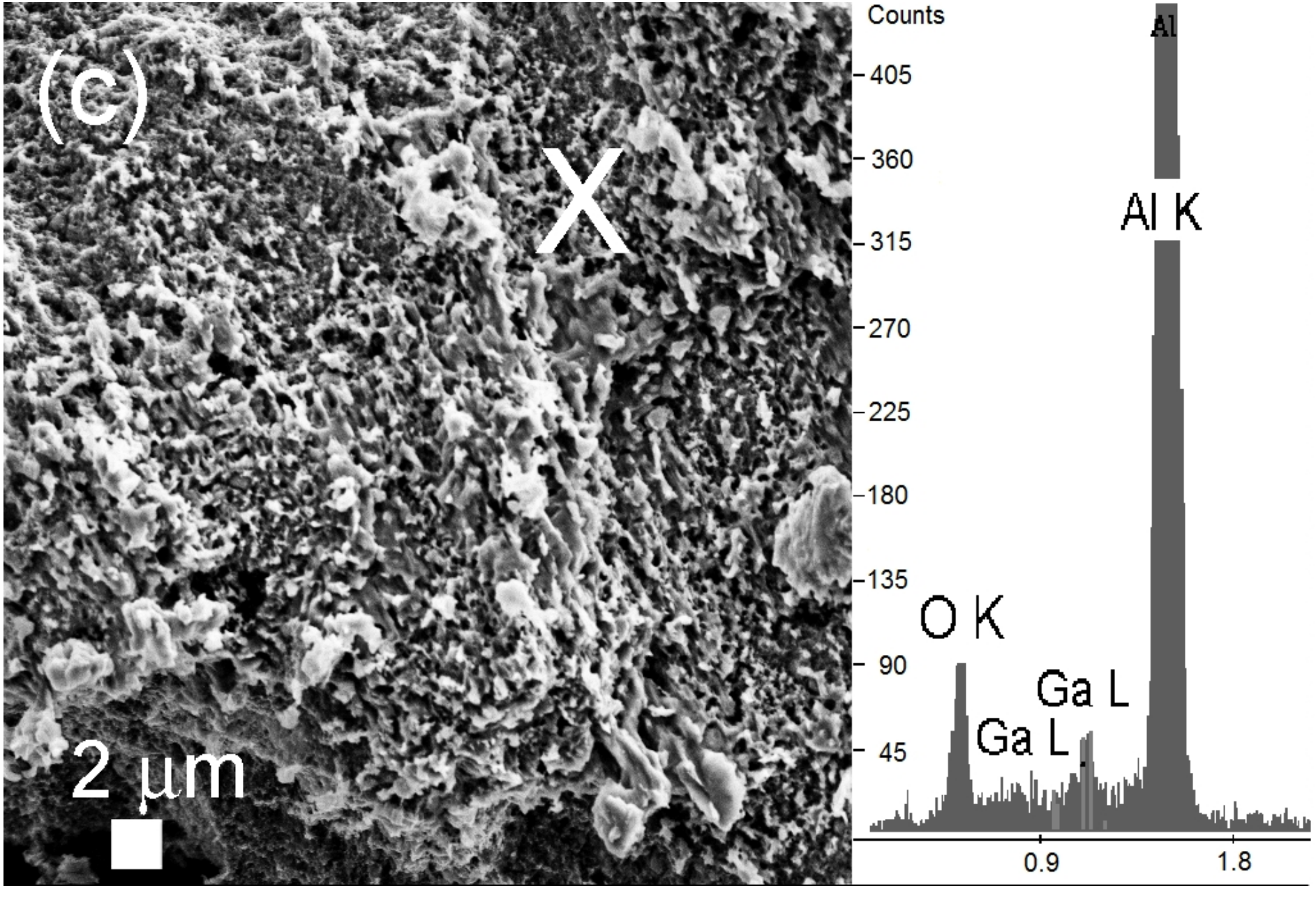
(c)
X
2 µm
Counts
405
360
315
270
225
180
135
90
45
Al
Al K
O K
Ga L
Ga L
0.9
1.8

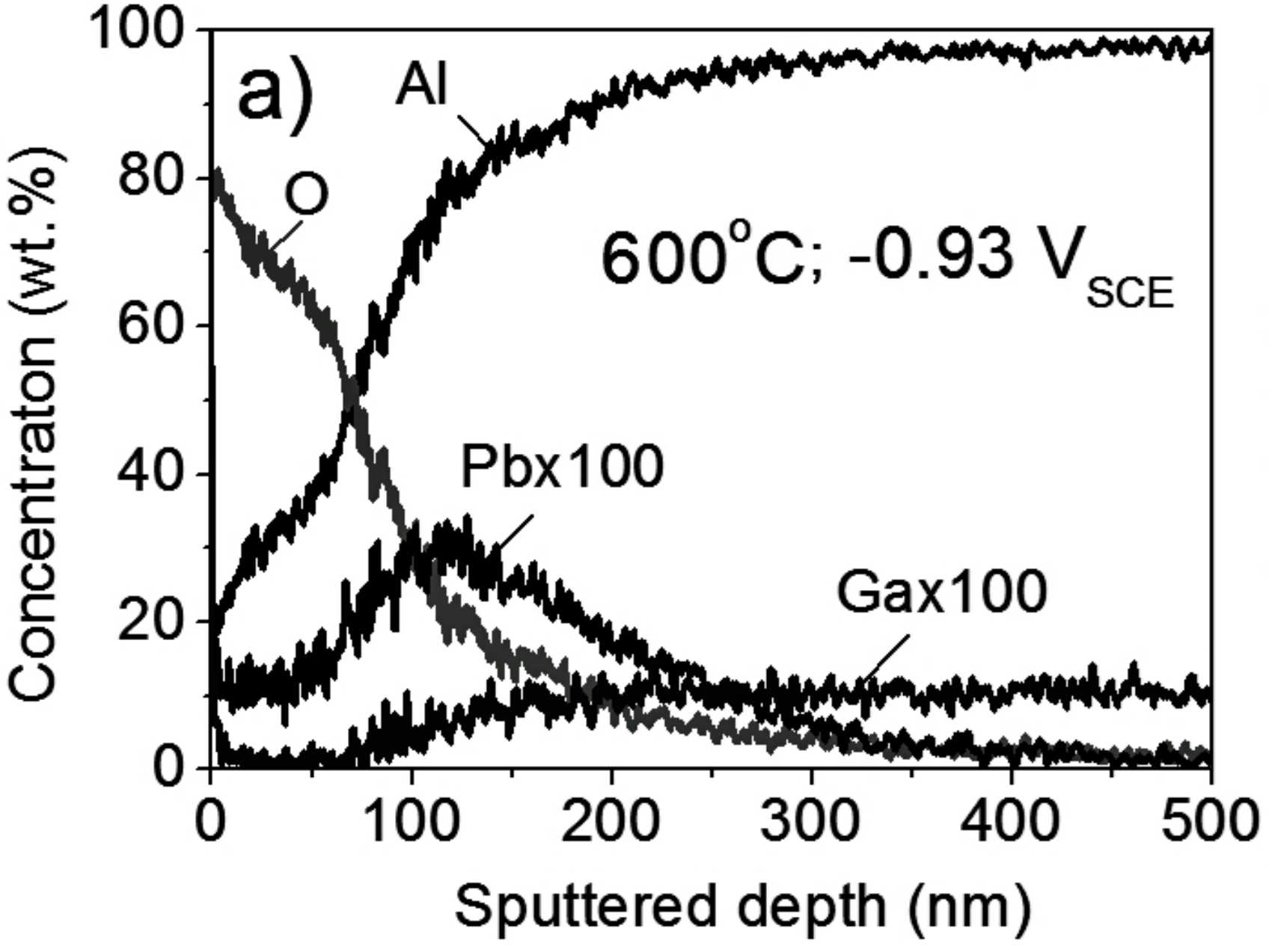
a)
Al
O
600°C; -0.93 V SCE
Pbx100
Gax100
Concentraton (wt.%)
Sputtered depth (nm)
0
20
40
60
80
100
0
100
200
300
400
500

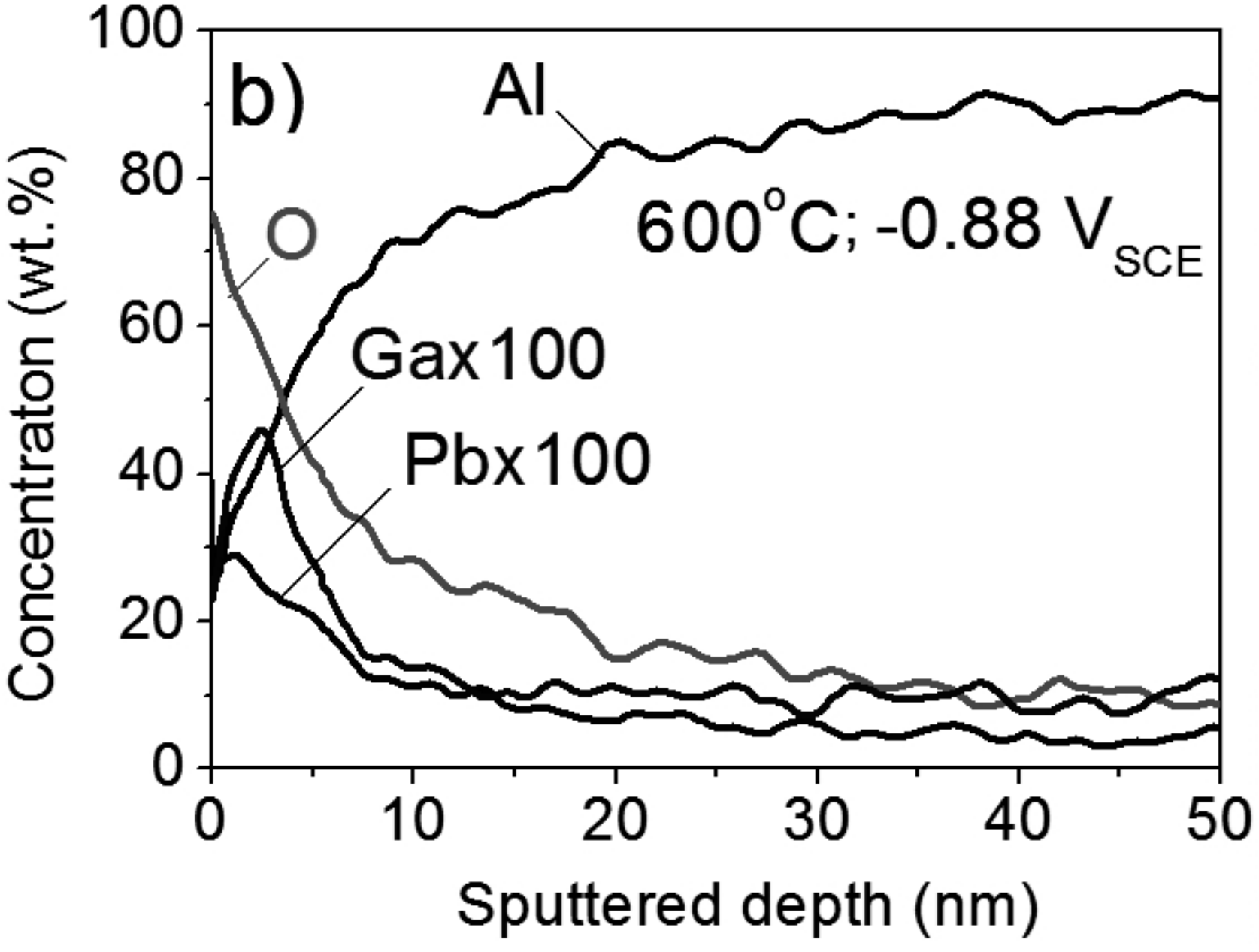
b)
Al
O
600°C; -0.88 V SCE
Gax100
Pbx100
Concentraton (wt.%)
Sputtered depth (nm)
0
20
40
60
80
100
0
10
20
30
40
50

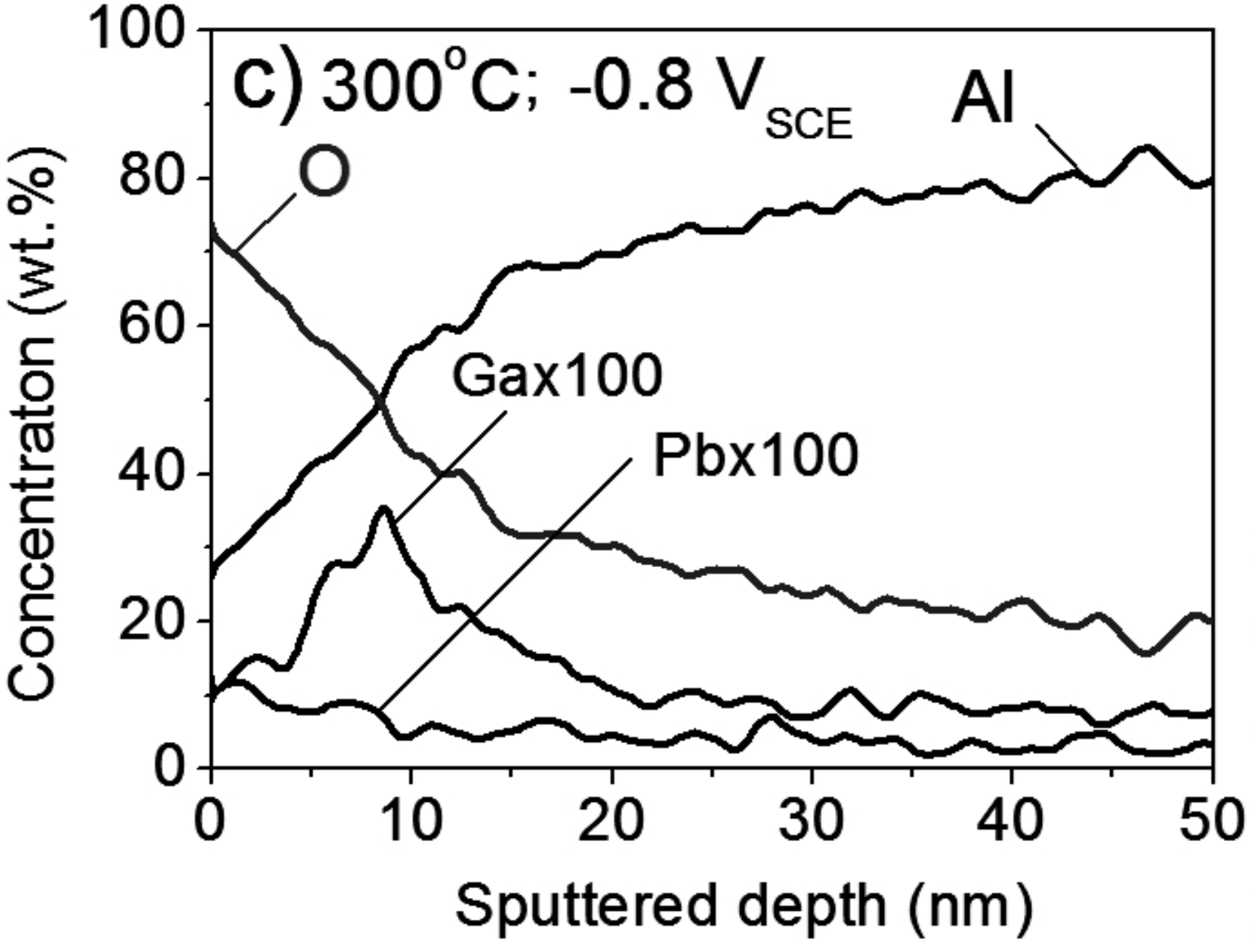
c) 300°C; -0.8 V SCE
Al
O
Gax100
Pbx100
Concentraton (wt.%)
Sputtered depth (nm)
0
20
40
60
80
100
0
10
20
30
40
50

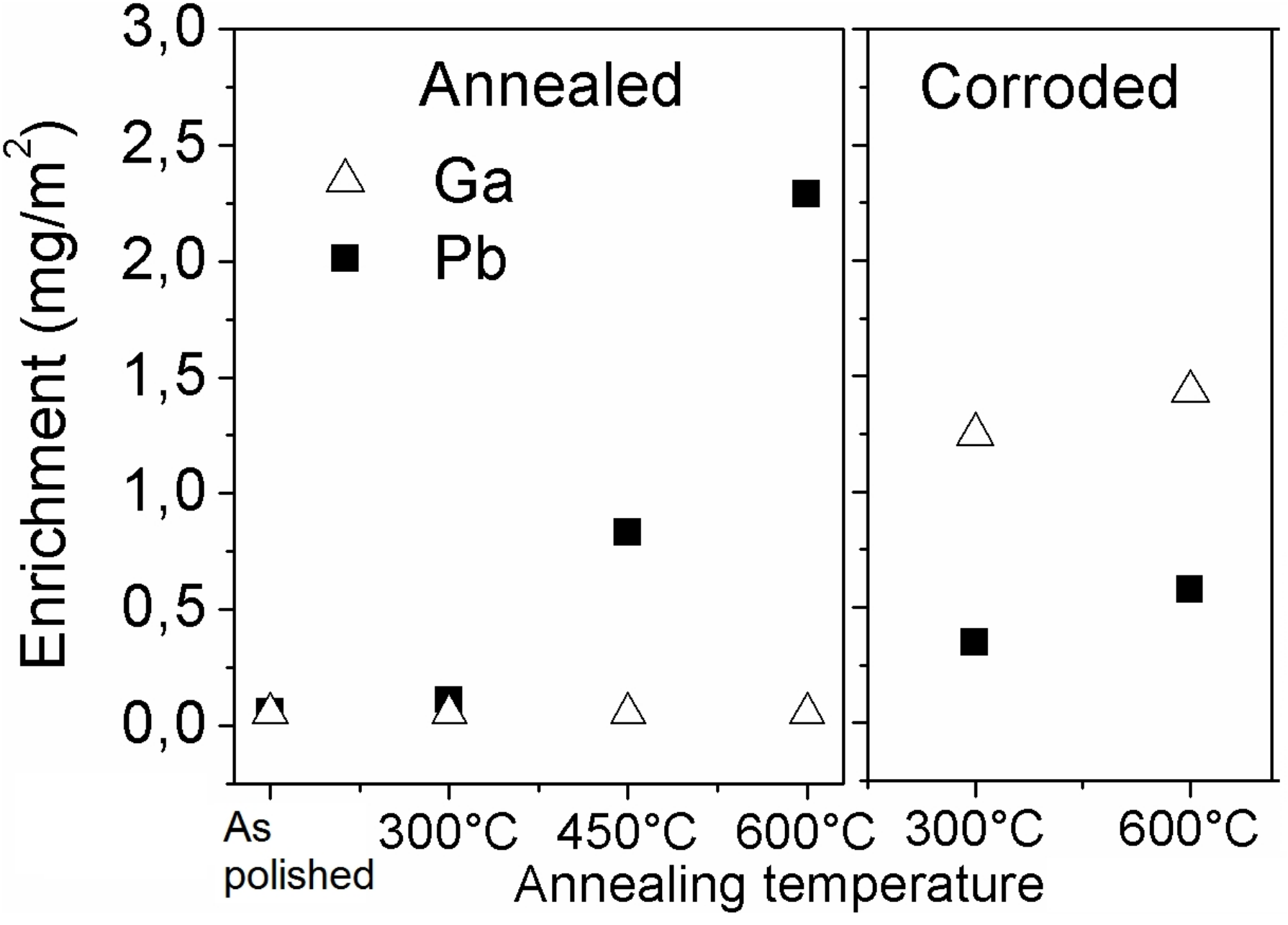
Annealed
Corroded
Ga
Pb
Enrichment (mg/m^2)
3,0
2,5
2,0
1,5
1,0
0,5
0,0
As polished
300°C
450°C
600°C
300°C
600°C
Annealing temperature